DESIGN AND SIMULATIONS OF MEMS BASED MICRONEEDLE ARRAYS FOR BIOMEDICAL APPLICATIONS

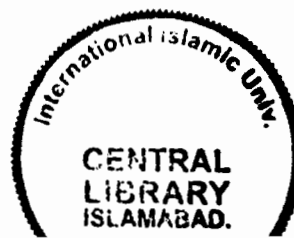**SUBMITTED BY**

NAME: FAISAL AMIN

REG NO: 226-FET/MSEE/S10

SUPERVISOR

PROF. DR. AHMED SHUJA SYED

ADVANCED ELECTRONICS LABORATORY

INTERNATIONAL ISLAMIC UNIVERSITY ISLAMABAD

FACULTY OF ENGINEERING AND TECHNOLOGY

2012

DESIGN AND SIMULATIONS OF MEMS BASED MICRONEEDLE ARRAYS FOR BIOMEDICAL APPLICATIONS

SUBMITTED BY
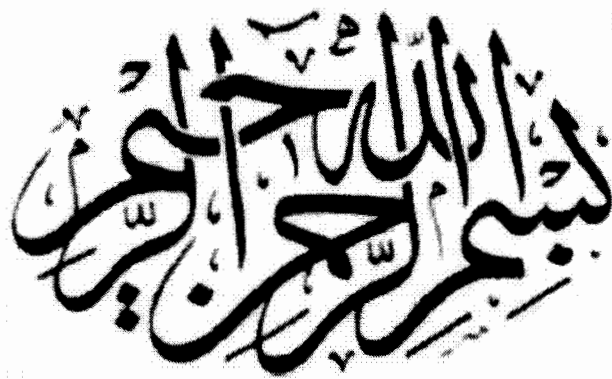**NAME: FAISAL AMIN**
REG NO: 226-FET/MSEE/S10

SUPERVISOR
PROF. DR. AHMED SHUJA SYED

Submitted in partial fulfillment of the requirement for
MS in Electronic Engineering with specialization in Advanced Electronics
at the faculty of Engineering and Technology, International Islamic University,
Islamabad

ADVANCED ELECTRONICS LABORATORY

INTERNATIONAL ISLAMIC UNIVERSITY ISLAMABAD

FACULTY OF ENGINEERING AND TECHNOLOGY

DEPARTMENT OF ELECTRONIC ENGINEERING

2012

بِسْمِ اللهِ الرَّحْمٰنِ الرَّحِيمِ

In the name of Allah, the most

Beneficent and the most Merciful

CERTIFICATE OF APPROVAL

Title of Thesis: Design and Simulations of MEMS Based Microneedle Arrays for
Biomedical Applications

Name of Student: Faisal Amin

Registration No: 226-FET/MSEE/S10

Accepted by the Faculty of Electronic Engineering, INTERNATIONAL ISLAMIC UNIVERSITY, ISLAMABAD in partial fulfillment of the requirements for the degree of Master of Science with specialization in Advanced Electronics.
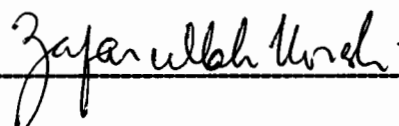
Viva Voce Committee

Dean
Prof. Dr. Mumtaz Ahmed
FET, IIUI.

Chairman
Dr. Muhammad Zubair
DEE, FET, IIUI.

External Examiner
Prof. Dr. Zafar-Ullah Koreshi
Dean, Faculty of Engineering
Air University, Islamabad

Internal Examiner
Dr. Ihsan-ul-Haq
Assistant Professor
DEE, FET, IIUI.

Supervisor
Prof. Dr. Ahmed Shuja Syed
Vice President
Academic Management & Outreach (CESET)
Islamabad.

Dedicated ....

To a Person who is "The Rehmat" for all the universe,

And

To our Parents and to whom we love and respect

Acknowledgement

First of all I am very thankful to Almighty Allah, The Kind and The Merciful, who gave me an opportunity to join the degree course of MS at FET International Islamic University, Islamabad and then make me able to complete this thesis work successfully.

I take immense pleasure to thank my Supervisor Prof. Dr. Ahmed Shuja Syed for providing me this opportunity to work under his supervision. I owe a great deal of gratitude to him and for the valuable guidance, encouragement, helpful advice, and timely suggestions rendered in the completion of this work.

I am highly indebted to my parents, brother and sisters for their patience and love. I am grateful to my parents for their prayers and love.

Finally, I would like to thank all staff in Advance Electronics Lab for their consistent support and love.

<div style="text-align:right">

FAISAL AMIN

</div>

TABLE OF CONTENTS

LIST OF FIGURES

LIST OF TABLES

ABSTRACT

In this study, modeling, design and simulations were carried out for "MEMS based silicon hollow out of plane" microneedle arrays for biomedical applications particularly for transdermal drug delivery. The fabrication process for these microstructures has been simulated on MEMS pro design tool. Symmetric and pointed shape microneedles have been designed with wide base that makes it robust for penetration into the skin. An approximate 200 μm length of microneedle has been formed by isotropic etching technique whereas the Deep Reactive Ion Etching (DRIE) has been exploited for 40 μm diameter of microneedle lumen. These microneedles are arranged in size of 2 x 4 matrix array with center to center spacing of 750 μm. Furthermore, comparisons for fluid flow characteristics through these microneedle channels have been modeled by ignoring and considering the gravitational forces (value of g) using mathematical models derived from Bernoulli Equation. Physical Process simulations have also been performed on TCAD SILVACO process simulator to optimize the design of microneedles.

INTRODUCTION

1.1 Introduction

The area of miniaturization and micro fabrication in the past few years changes tremendously in numerous engineering and scientific fields due to extensive preponderance progress in micro electromechanical systems (MEMS) and Microsystems. The micro electromechanical systems (MEMS) based devices for biomedical applications referred as BioMEMS is an emergence "small scale" field which has been specified to the living systems [1]. The BioMEMS based devices increase its efficiency and robustness with the advancement of technology in both micromachining tools and design structure [2].

Sampling and extraction of biomolecules and fluids, drug delivery, therapeutics and diagnostics etc are the major areas of biomedical industry where MEMS based microstructures have been successfully implemented and more research is still in progress to connect miniaturized products with the biological environment [1]. Biocompatibility and broad protocols of experiment procedures are primarily required for the manufacture of biomedical microstructures [3].

Potential advancement and improvement in micro fabrication technology has made it convenient to transport specific biological fluid into or out of human skin with minimum discomfort [2, 4]. Fluid transdermal delivery systems such as Microneedle arrays are one such emerging and exciting microsystem which could be able to penetrate and manage a control amount of biological fluid into the skin painlessly. Thus microneedle arrays offer great application and advantage over conventional needles.

Microneedles have been developed for different applications with different variety of materials [5], fabrication techniques [6], design [7], dimensions [8] and tips shape [9] etc. In this thesis an approach has been made to design and simulate fabrication steps for microneedle arrays for biomedical applications that would be hollow and out of plane in structure.

1.2 Objective of the Study

The objective of this study is to design and simulate "hollow" and "out of plane" microneedle arrays for bio-medical applications using different MEMS and device processes along with geometries. The design, analysis and simulations of microneedle arrays were carried out on a commercially identified IP protected MEMS PRO Design software and SILVACO ATHENA process simulator available in Advanced Electronic Design Suite in the faculty.

1.3 APPROACH AND METHODOLOGY

- Literature were studied to compile a database on all possible design and process routines used to study such devices for bio-medical applications;
- Selected design routines were implemented on MEMS design tool to analyze the design-specific characteristics;
- A suitable Silicon substrate along with all the required MEMS-specific engineering properties were chosen to design the devices after the analysis made on various geometries and their mechanical dynamics of the microneedles;
- Several runs of simulations were made in order to use the optimum process routines to design the devices for a certain application;
- Post-finalization of the process routines were maintained on MEMS pro to ensure a final (corrected) design of the devices;
- Physical based simulations were carried out on SILVACO ATHENA process simulator for selection of the appropriate available processes parameters for the optimize design of microneedles;

1.4 Thesis Overview

- ➢ With an introduction in this chapter; Chapter 2 explains the MEMS and Microsystems applications in various industries especially focus on biomedical industry with examples.

- ➢ Chapter 3 describes about the microneedles with their history, applications and geometry and brief description of skin anatomy, which is important to understand for the optimization of design.

- ➢ In Chapter 4 the literature that has been reviewed for microneedles is presented.

- ➢ Chapter 5 discusses the basis of the model to identify the fluid flow characteristics through microneedles where mathematical models have been derived from Bernoulli Equation and remodeled to satisfy our design consideration.

- ➢ Chapter 6 concentrates on design and fabrication process steps of the microneedles that has been simulated on MEMS Pro design tool and summary of the comparison also has been presented between the fabrication process simulator and general fabrication parameters and techniques for microneedles fabrication.

- ➢ Chapter 7 illustrates the process simulation steps for microneedle that has been simulated on SILVACO ATHENA process simulator along with other optimized parameters that might be helpful in microneedles fabrication process.

- ➢ Chapter 8 presents the results obtained on the work described in chapters 6 and 7, along with the discussion.

- ➢ Chapter 9 sheds light on the summary of the work carried out along with major findings and some ideas about futuristic work that may be considered in continuity.

MEMS AND MICROSYSTEMS

2.1 Micro Electro Mechanical Systems (MEMS)

Microelctromechanical systems is defined as:

"Microelectromechanical systems, or MEMS, are integrated micro devices or systems combining electrical and mechanical components, fabricated using integrated circuit (IC) compatible batch processing techniques and varied in size from micrometers to millimetres. These systems merge computation with sensing and actuation to change the way we perceive and control the physical world" [10].

Generally, MEMS composed of microsensors, microelectronics, microactuators and mechanical microstructures are incorporated on similar silicon chip [11] shown in Figure 1. MEMS elements have the capability to combine together to achieve complex microscopic tasks in large arrays or work individually to achieve sophisticated results.

Some of the well knows industries such as medicine, automotive, telecommunications and aerospace are increasingly using MEMS components such as Gyroscope and airbags in automotive industry, biosensors, implantable chip, microneedles and surgical devices in medicine and biomedical industry, IR microoptics and RF waveguides in telecommunications and micro Unmanned aerial vehicles (UAVs), Manifold absolute pressure (MAPs), arm in aerospace industry [12].
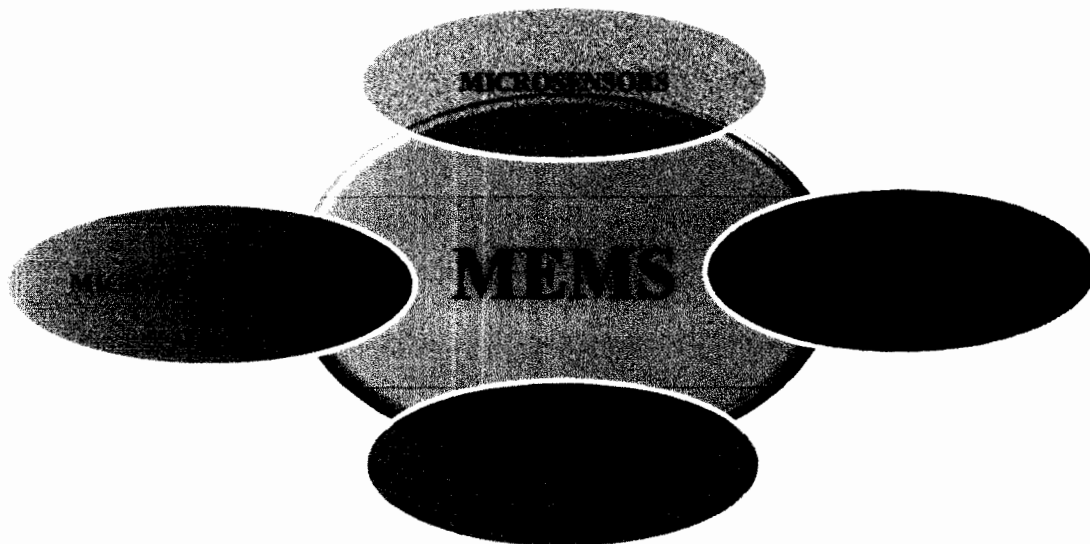
Figure.1 MEMS Components [11]

The thermal, electrical, magnetic, chemical, mechanical or biological signals or information are received by the microsensors [11, 13] and ultimately detect alternation in the environment of the system. This signal or information is then executed by the processing unit and signal transduction of the microelectronics which is then converted into forms that are companionable with the microactuator to generate and response some sophisticated alternations to the environment [14]. It means that the MEMS at the miniaturize level control and direct physical parameters by amalgamation of sensing and actuating functions.

2.2 MICROSYSTEM

A microsystem is defined as:

"A microsystem (MST) is defined as an intelligent miniaturised system comprising of sensing, processing and/or actuating functions. These would normally combine two or more of the

following: electrical, mechanical, optical, chemical, biological, magnetic or other properties, integrated onto a single or multichip hybrid" [15, 16].
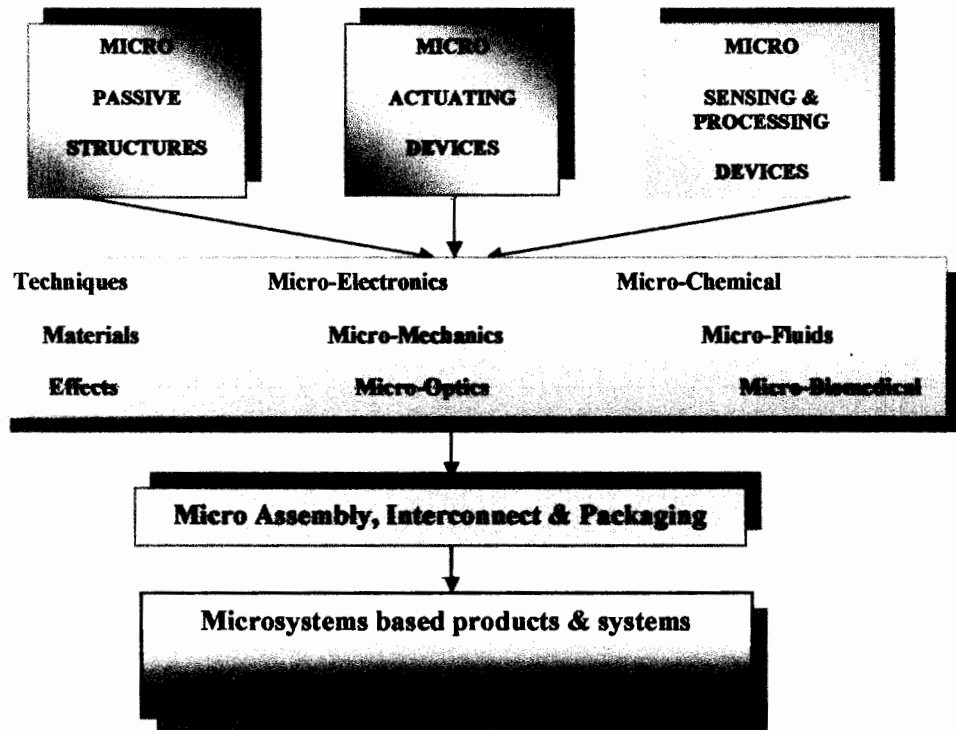
Figure.2 Microsystems in a complete application system [17]

MEMS components are contained in a micro engineering system which is designed in such a way to deliver targeted engineering tasks and functions [14]. As shown in figure 2, this amalgamation of functionality encompasses micro actuating devices such as high precision microoptics, micromechanics, microelectronics, microbiomedical etc. Microsystems also have great affiliation to components of integrated circuits in lieu of fabrication techniques and materials and their high level integration [18].

2.3 Salient Features of MEMS and Microsystems

The diverse field of MEMS and Microsystems and its devices provide some of the following features [11, 13]:

(a)   Enhance reliability, functionalities and capabilities from engineering perspective;

(b)   Batch production in batches provides low manufacturing costs;

(c)   Miniaturization substantially reduces the weight, volume and size;

(d)   Consumption of very low power;

(e)   Dominant in every aspect of market place;

(f)   Size reduction causes simple integration into systems which increases applicability;

(g)   Combines the principles of many engineering and natural science disciplines;

2.4 Categories of MEMS

The area of MEMS is generally divided into following categories that are [19, 20]:

(a)   Microsensor;

(b)   Microactuators;

(c)   Micro optical electromechanical systems (MOEMS);

(d)   Radio frequency Micro Electromechanical Systems (RF-MEMS);

(e)   Biological Micro Electromechanical Systems (BioMEMS);

The MEMS categories and their functions with examples are listed in the table 1:

Table.1 MEMS Categories and its Functions

S.NO	MEMS CATEGORIES	FUNCTIONS	EXAMPLES
1	Microsensors	Perceive environment	Thermal, acoustic wave, optical, biomedical, chemical, pressure and bio sensors [14, 19]
2	Microactuators	control the environment	Micropumps, micromotors, microgrippers, microvalues, microaccelerometers [14]
3	MOEMS	Reflect, diffract or refract light	Optical switches, reflectors [19] Microlens arrays, IR optics, diffusers [21]
4	RF MEMS	Emphases on switches and transmission of high frequency	metal contact switches, shunt switches, tunable capacitors, antennas [19]
5	BioMEMS	Processing, delivery, manipulation, analysis, or construction of biological and chemical entities[10]	Microneedles, microsyringe, pacemakers, disposable BP tranducer, Lab on chip systems[22], viscometric sensor for glucose monitoring [23]

2.5 Applications of MEMS and Microsystems

The following sections describe the applications of MEMS and Microsystems in various industries:

2.5.1 MEMS Applications in Defence and Aerospace

Application of MEMS In Defence and Aerospace is summarized in table 2:

Table.2 MEMS Applications in Defence and Aerospace

DEVICES	FUNCTIONS	REFRENCES
Digital Micromirror Device (DMD)	Display projection images	[24, 25]
Micro, Unmanned Aerial Vehicles (UAVs)	Deploy micropay loads	[24, 25]
Manifold Absolute Pressure (MAP) sensor	Compute the amount of fuel required	[24, 25]
Sensors and actuators	Fuel measurement and monitoring, landing gear, ice protection, and navigation	[24, 25]
Micro optics and micro mirrors	Laser communications	[14]
Microsatellites	Space Communications	[14]
Space environment sensors	Gravity gradient monitors	[14]
Chip thermal switches and MEMtronics	Control and command systems	[14]

2.5.2 MEMS Applications in Optics and Telecommunications

Applications of MEMS in optics and telecommunications are given in table 3:

Table.3 MEMS Applications in Optics and Telecommunications

DEVICES	FUNCTIONS	REFERENCES
Optical Microphone arrays	Signal processing algorithms, Directional sensing	[26]
Low-G inertial sensor	Seismology , Geolocation and Navigation	[26]
Nanophotonic Optical Transducers	Displacement Sensing	[26]
Optical modulator	Chemical identification	[27]
Optical Device for Maskless Exposure Systems	Semiconductor production process engineering	[27]
Microlens arrays	Optical Switches, Amplifiers, and Isolators	[28]
IR microptics	Night Vision Enhancement, Weapon Sight	[28]
Two axis tilt mirrors	Photonic switches, Retinal scanning system	[28]

2.5.3 MEMS Applications in Automotive

There are mainly four major areas in automobile where the MEMS and Micro systems are categorized [16] that are

(a) Saftey;
(b) Engine and power train;
(c) Comfort and convenience;
(d) Vehical diagnostics and health monitoring;

Some of the MEMS devices used in automotive industry are given in table 4:

Table.4 MEMS Applications in Automotive

DEVICES	FUNCTIONS	REFERENCES
Airbags	Crash sensing	[27]
Automatic Headlight Leveling	Accelerometer used for tilt sensor	[27]
Silicon microphone	Hands-free Communication	[27]
Gyro sensor	Global Positioning System	[27]
Manifold Absolute Pressure (MAP) Sensor	Engine control	[27]
Seat belt pre-tensioner system	To lock the seat belt during a crash	[27]
Accelerometers	Seat belt pre-tensioner system	[27]

2.5.4 MEMS Applications in Biomedical

Application of MEMS in biomedical industry is given in table 5:

Table.5 MEMS Applications in Biomedical

DEVICES	FUNCTIONS	REFERENCES
Biomedical Microsensors	Biomechanics, Pneumatic, Chemical and electrical Biosystems, Impedance and molecular specific sensors	[11]
Biomedical Microactuators	Micromanipulations, Microvalve, Micropumps, Microfilters	[11, 14]
Adaptive Rate Pacemaker	Sense exertion and Regulate heart rate	[27]
Implantable chips	Timed Drug Delivery	[27]
Blood Pressure Monitor	Sense pulse rate	[27]
Insulin Nanopump	Miniaturized insulin delivery system	[27]
Catheters	Pressure and Flow measurement	[27]
Ventilators, Respirators	Oxygen and Respiratory flow sensor	[14]
Retinal implant	Provide the sense of vision	[14]
Microneedles	Trandermal drug delivery, Trandermal blood extraction	[14]

2.6 Biological Micro Electro Mechanical Systems (BIOMEMS)

BioMEMS is defined as:

"Devices or systems, constructed using techniques inspired from micro/ nano-scale fabrication, that are used for processing, delivery, manipulation, analysis, or construction of biological and chemical entities" [1].

This category of MEMS not only finds its place in rapid advanced biomedical and medicine research area but its devices are now commercially available globally [29]. BioMEMS as a whole at micro scale integrates many biomedical systems and biological sciences disciplines and applications, as shown in figure 3, where one side identifies the biomedical and biological problems research area for the applications of micro and nano systems and opposite side illustrates the molecular effects of biological sciences applications to the materials of micro and nano systems [1].
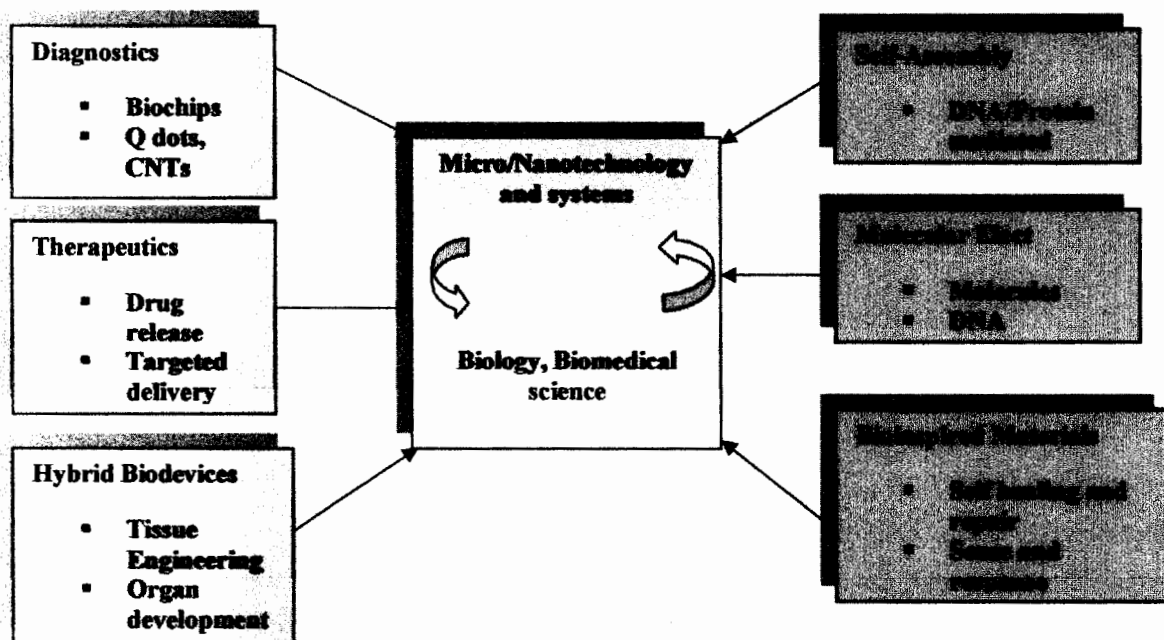
Figure.3 Research and Development areas of BioMEMS [1]

2.7 Examples of BioMEMS

This section belongs to the description of two major areas where BioMEMS are employed on commercial and procedural basis:

2.7.1 Biomedical Implants

2.7.1.1 Cochlear Implant

Cochlear implant is an electronic complex bio device where one part of the device is invivo beneath the skin surgically whereas other part is externally placed, used by the persons who are hard of hearing [30, 31]. The biomedical implant provides the individuals with good understanding of speech and sound environment by directly stimulate and activate the auditory nerve [30].

Cochlear implant is an integration of electrode array, speech processor, microphone, transmitter and receiver stimulator [30, 31], as shown in figure.4.
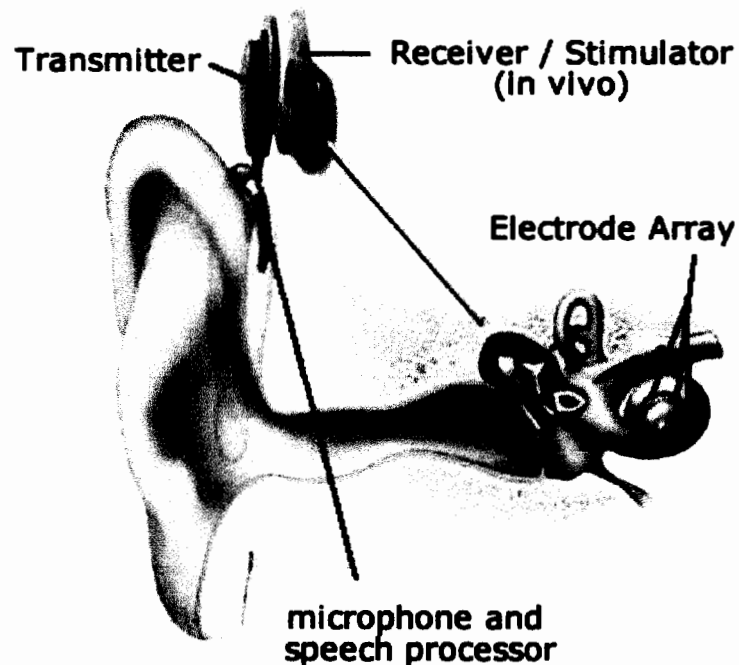
Figure.4 Cohlear Implant [31]

2.7.1.2 Retinal Implant

The retinal prosthesis is stunning potential implant device that functions to provide the sense of vision for patients with blind diseases caused by the photoreceptors cells of the outer retina of the eye [32, 33] as shown in figure 5. Several other designed approaches have also been developed such as optic nerve, subretinal, epiretinal, cortical visual stimulations [32, 33]. These prosthesis systems have been developed due to technology advancement in BioMEMS techniques and their controlled circuitry integration.
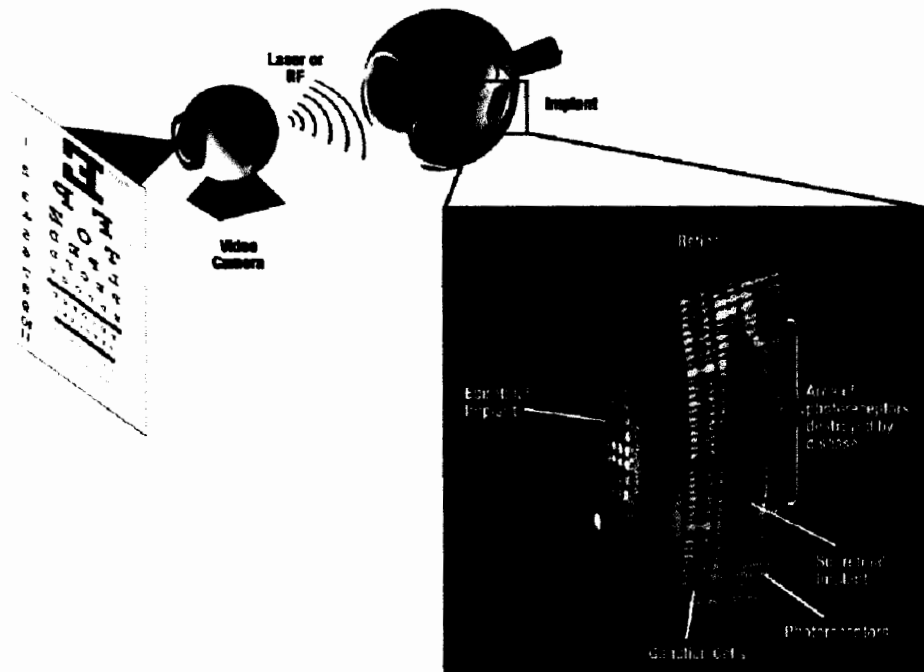
Figure.5 Retinal Prosthesis Implant [32, 33]

The retinal implant device activates the bio electrical signals of the nerve cells which in turn results in restoration of vision [32, 33]. The retinal implants placed in the eye receive the information that is transmitted by the processing system after bioelectrical signal are converted by the light [32, 33]. The electrode array, which is occasionally positioned on the retina surface, deliver the artificial stimulus which is received and produced by the secondary systems of the implant [32, 33].

2.7.2 Biosensing and Transducing Elements

Biosensors are the integration of an analytes , bioreceptors, transducer and readout devices [34]. The analyte combines with bioreceptors which are sensing element that provides such a physio-chemical effects produced by targeted bio species that is quantitatively detectable and measureable by transducer which read out the results in the form of bioelectrical signals [34]. Advances in microfabrication technology leads to the development of many sophisticated BioMEMS sensors and tranducers for many clinical applications, few of which are shown in figure 6.

Sub-μm
(Proteins, DNA)

Surface Acoustic Wave
(Proteins)

Polermert Els
(pH, glucose)

Magnetic-bead
Biosnsor (Proteins, DNA)

Transmission Plasmon
Biosensor (Proteins, DNA)

GaAs MESFETs
(neurons, proteins)
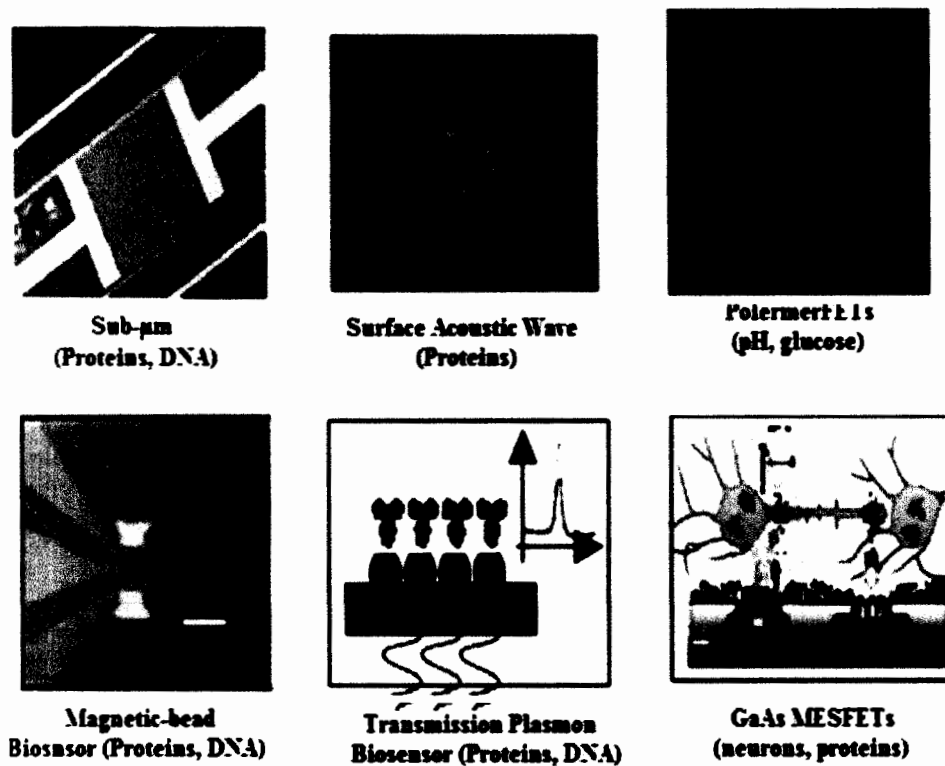
Figure.6 Different Biosensors and Tranducers [35]

There are several detection modalities which are used by BioMEMS sensors, including the mechanical, electrical and optical detection [1]. Biosensors mainly detects biomolecules entities such as DNA, polypeptides, proteins, cells, nucleic acids, enzymes, microrganisms and many other small biomolecules [1, 34].

These days biosensors are arrays or integration of individual biosensors to detect many biomolecules and biochemical processes and they further analyze analytical capabilities which rapidly leads to the applications of clinical diaganostics on single microchip which is sometimes called biochips [1, 34, 36] as shown in figure 7 (a & b), used for clinical diagnostics [36].
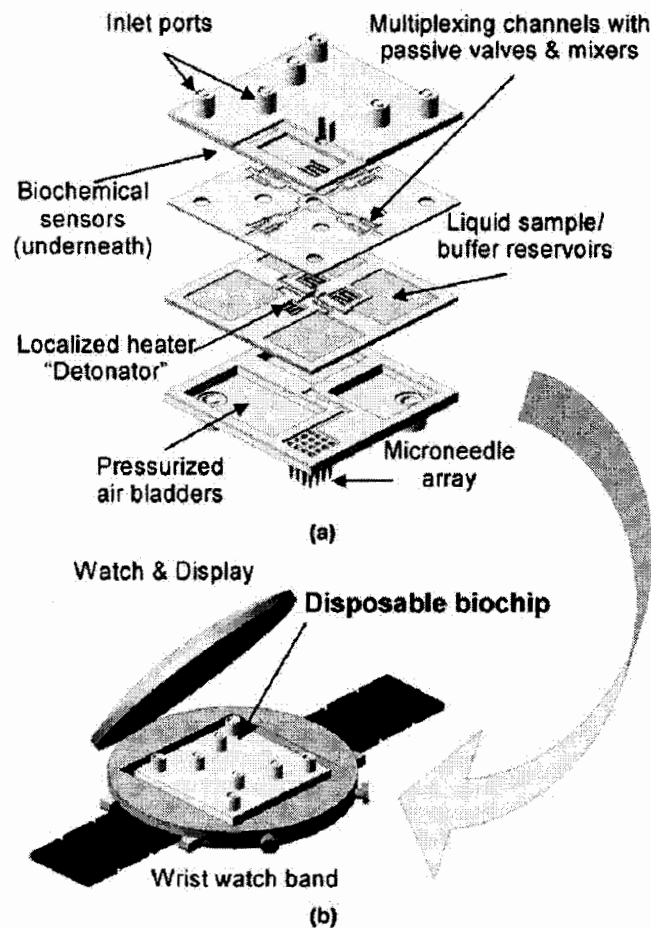
Figure.7 (a) Multilayer Development of Disposable Biochip [36] (b) Biochip with Wristwatch Sized Analyzer [36]

17

MICRONEEDLES AND THEIR USAGES

3.1 Brief History of Microneedles

Patients have been delivering drugs through hypodermic needles for about 160 years [4, 38]. For the transdermal drug delivery and transdermal blood extraction hollow needles have played a very vital role since they were manufactured in 18th century and later shortly first injection was then administered [4, 38].

In the mid of 1970s the Alza corporation [38] presented the concept of using microneedle for the administration of drug delivery on the skin but until 1990s it was experimentally not shown due to unavailability of microfabrication techniques [39]. In the end of 1990s microneedles become the stunning research area of MEMS and different shapes and materials were used for their fabrication [40-43].

The first microneedle arrays were developed by etching the silicon wafer for intracellular delivery reported in the literature [39, 40]. To increase molecular uptake and gene transfection these needles were inserted into cells and nematodes [39, 40]. The improvement of transdermal drug delivery was carried out for the first time which caused skin permeability to a small model compound by inserting the microneedle in cadaver skin [41]. In 1991, the foremost out of-plane microneedle array, consisting of 100 microneedles with a length of 1.5 mm was reported [44].

In last decade more tremendous approaches and methodologies have been made in the development of microneedles for transdermal drug delivery and transdermal blood extraction and many other biomedical applications with different MEMS processing techniques, sizes, materials and shapes [2, 45-48].

3.2 Microneedles: Advantages and Applications

For the very purpose of the extraction of biological fluid and drug delivery for skin permeability, the BioMEMS based microneedle array technology provides many advantages and applications over conventional needles, including [49, 50]:

a) The length of microneedle can be controlled for the precise parenteral injection of therapeutic agents, by considering skin anatomy;

b) It is minimally invasive, due to smaller diameters at the tip;

c) Microneedles are arranged in arrays in order to transport large volume of fluid and penetrate invivo the skin over large distributed area rather than using single needle [8];

d) Provide painless drug delivery due to the fact that microneedles do not reach the nerves deep below the skin;

e) Single wafer is being used for the fabrication of arrays of microneedles due to its small size which tends to be a good design metrics including reliability, biocompatibility, fabrication cost, accuracy and etc [4, 50];

f) BioMEMS based microneedles array devices also find its application tremendously in biomedical sciences such as:

(a)   Treatment of cancer;

(b)   DNA transportation;

(c)   Introducing biomolecules in living cell;

(d)   Diabetes;

g) A microneedle array has been applied to the measurement of trandermal skin potentials in human subjects and these potential charges were recorded in the vicinity of superficial wounds confirming the generation of a lateral electric field in human skin reported [31];

3.3 Geometry of Microneedles

3.3.1 Types of Microneedle

The following section describes the types of microneedles, normally being used both in R&D and commercially:

3.3.1.1 Out of Plane and In-Plane Microneedles

Based on the fabrication process techniques microneedles are classified into two types shown in figures 8 (a & b):

(a)   Out of plane microneedles

(b)   In-plane microneedles

In out of plane microneedles, the structure of the flow channel and shaft is normal and protrudes out of the surface of the wafer substrate [7,8,39,41,43,47,48,50,53,54]. In in-plane microneedles, the structure of the flow channel and shaft is parallel and in plane to surface of the wafer substrate [7,8,39,41,43,47,48,50,53,54].

(a)   (b)
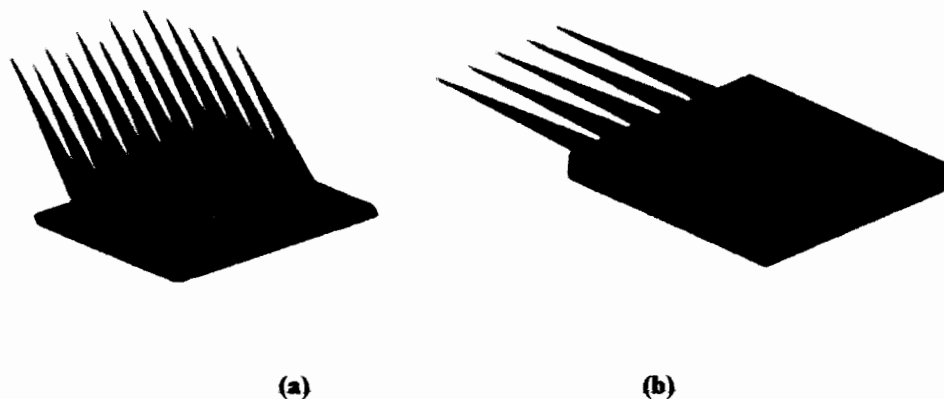
Figure.8 (a) Out of Plane Microneedles   (b) In-Plane Microneedles

Out-of-plane microneedles are very robust and these microneedles have capability to flow the fluid volumetrically as they are two dimensionally fabricated [50]. The major disadvantage of

out of plane microneedles is that it is defined by process of deep removal which becomes hard to control and makes them expensive as well as time consuming [50]. On contrary, In-plane microneedles lengths are easy to control and these in-plane structures are fabricated when the substrate material are etched away under the microneedles, which consequently makes them restrain to one dimensional arrays [50].

3.3.1.2 Hollow and Solid Microneedles

With reference to the physical structure microneedles are also comprises of two types shown in figure 9 (a & b) that are:

(a)   Hollow microneedles
(b)   Solid microneedles

Hollow microneedles are the microneedles that direct the flow of biological fluid and drugs through its internal lumen [7,8,39,41,43,47,48,50,53,54]. Solid microneedles are the microneedles in which either the lumen surface is coated with particles of drugs and applied to the skin or since the base of solid microneedles is non dissolving it is sequentially removed after the dissolution of microneedles [7,8,39,41,43,47,48,50,53,54].

(a)   (b)
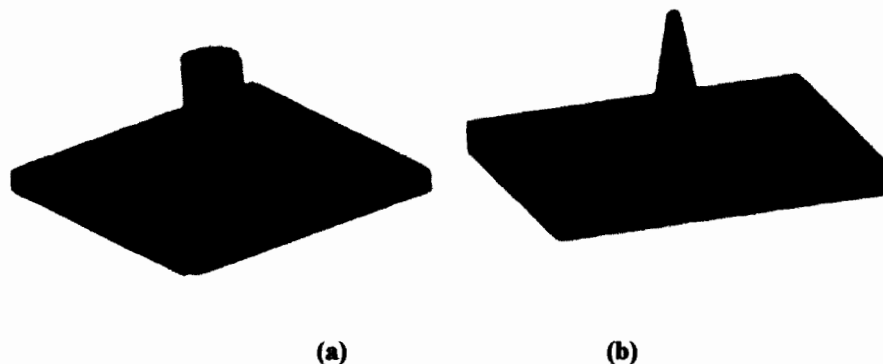
Figure.9 (a) Hollow Microneedle   (b) Solid Microneedle

For continuous transportation of drugs into the body, BioMEMS based hollow microneedle arrays are properly used either by pressure driven pump or by diffusion which is mostly using transdermal drug delivery systems in biomedical applications [50]. For transdermal blood extraction hollow mcironeedles are also used by increasing the appropriate length of needle shaft. Solid microneedles on the other hand allow diffusion rates and permeability to rise and also available in form of drug coating [50].

3.3.2 Shape and Materials of Microneedles

The factors such as skin permeability and penetration along with the strong biocompatibility require an appropriate shape and selection of materials of the microneedles which is very critical during the process of fabrication and design. Any specific applications particularly in biomedical sciences, the selection of both shapes and materials is very important simultaneously. The shape of microneedles can be categorized into two types with respect to the Overall shape and Tip shape. Table 6 summarizes various designs of microneedle shapes and materials:

Table.6 Lists of Shapes and Materials of Microneedles

OVERALL SHAPE	Pyramidal, Spear, Candle, Cylindrical, Spike
TIP SHAPE	Tapered, Beveled, Snake fang, Volcano, Canonical
MATERIAL	SU-8, Silicon, Metals, Polymers, Silicon dioxide, Glass

3.4 Skin Anatomy

The better understanding of skin structure is very much required for small scale fabrication of needle arrays. The human skin is the most multifunctional and largest organ of the body that interacts with the surrounding world [55]. The stratified structure of skin consists of three main layers that are epidermis, dermis and hypodermis as shown in figure 10.
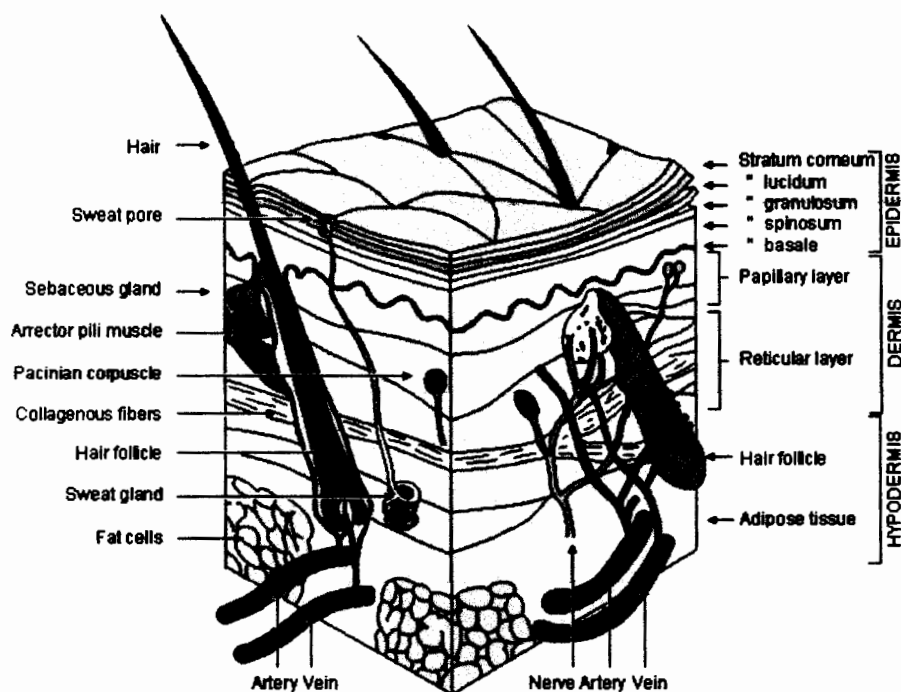
Figure.10 Anatomy of Skin [56]

3.4.1 Epidermis Layer

The superficial epithelium layer epidermis is approximately 50-150 μm thick which largely consists of cells called keratinocytes [45] which are formed in the basal layer of epidermis [55]. The epidermis layer also constitutes melanocytes, langerhans cells and merkel cells [55, 57]. Epidermis is further subdivided into five layers i-e stratum corneum, Stratum lucidum, stratum basale, stratum spinosum, stratum granulosum [55, 57]. The major barrier for drug

delivery is the stratum corneum which is about 10 to 20 μm thick [57] is the outermost layer of the epidermis adherently consists of stacked cornified cells of hexagonally flat shape [45, 55, 57]. The deepest layers of the stratum corneum contain lamellar granules that act as major part of the permeability layer [55, 57].

3.4.2 Dermis Layer

The dermis is the second thick layer distributed with connective tissues [55]. The dermis is further subdivided into two regions i-e the first level called papillary region consists of loose connective tissue and small collagen fibers while the second level called reticular region constitutes closely packed tissue and constitutes the bulk of dermis [55, 57]. The dermis is mainly consists of elastin, network of blood vessels and capillaries and collagen matrix [55, 57]. The work assign to the capillary network is to supply nutrients to different skin layers, the elastin maintains elasticity of skin and strength to the skin is provided by collagen fibers. Although the dermis comprises of rich blood supply network but no blood vessels pass the dermo-epidermal junction [55].

3.4.3 Hypodermis Layer

The hypodermis also called subcutaneous fat is a fatty layer which is attached loosely to the superficial dermis [55, 57].

So, the structure of skin offers the great opening for the transdermal drug delivery as well as drug absorption [58]. The microneedle fabricated should therefore not reach the dermis but it may tend to penetrate the stratum corneum into epidermis of the skin. This suggests that for transdermal drug delivery, the length of microneedle fabricated must be in range of 150 – 250 μm size [58].

LITERATURE REVIEW

The literature has been surveyed to form the basis of studies relevant to our work particularly with reference to the microneedle geometry, dimensions and different fabricating techniques, alongwith the focused application area. The design and process sequences are of great importance and hence they are particularly highlighted in the survey.

4.1 Literature Survey

Po-Chun Wang et al [59], exploit UV photolithography and micromolding technique to manufacture the hollow microneedle array with side open lumen and beveled sharp tips patch polymer for drug delivery [59]. Figure 11 shows the fabrication processes steps for hollow microneedles [59]. The geometry of the hypodermic needle consists of needle length of 1mm, open sides with lumens with a diameter of 150 µm, an array size of 6 x 6. Liquid Features indicate that at least 85% of the lumens were open and the overall flow was 2 ml / minute [59]. Tests conducted during this study showed successful enrollment rates of 97 percent and no apparent damage after registering microneedles [59].
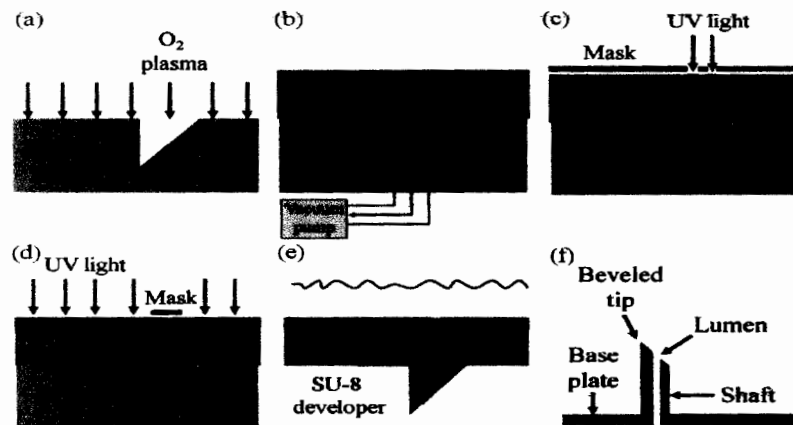
Figure.11 Fabrication Processes Steps for Hollow Mironeedles [59]

Jooncheol Kim et al [6], conducted a study with different geometries and the high aspect ratio of microneedles demonstrated by representatives of drug loading amount of controllable mechanical strength [6]. These microneedle arrays were formed by combination of micromolding and direct drawing rather than by using etching or lithography process [6]. Needles of biocompatible polymers were formed with water soluble, but the process of construction inherently allowed the exploitation of several kinds of polymers [6]. The modified microneedle had a shaft length of 800 μm with neck diameter of 240 μm arrayed in 10 x 10 matrix [6].

Muhammad Waseem Ashraf et al [48], employed Inductively coupled plasma (ICP) etcher for the fabrication of array size of 5 x 5 silicon out of plane hollow microneedles having length 200 μm with inner and outer diameter of 60 μm and 150 μm respectively with fluid reservoir at the back side [48]. These analyses provided the successful results for the effect of mechanical properties and stress distribution on silicon microneedles with maximum stress of 5.05 GPa and these results were found to be in secure range of predictions [48].

Buddhadev Paul Chaudhri et al [60], fabricated polymer material SU-8 based, cylindrical out of plane hollow microneedle arrays for transdermal drug delivery and extraction of blood [60]. This was done by technique of Deep Reactive Ion etching (DRIE) with dimensions of very high length of 1540 μm shaft along with inner diameter of 100 μm and a 15 μm wall thickness having extreme high aspect ratio of 103 with shapes of different cross sections [60]. It was revealed in this study that the mass production is only possible after many effective repeatable processes [60]. Microneedle insertion test was performed and it was found that insertion force caused no real damage to the microneedle as penetration into skin was satisfactory with given wall thickness [60]. Moreover, during the manufacturing process tradeoff was noticed with SU-8 small structures [60].

D.W. Bodhale et al [7], designed and fabricated tapered tip cylindrical silicon hollow microneedle arrays by using the technique of deep Reactive ion Etching (DRIE) followed by collective sequence of isotropic and anisotropic etching processes [7]. Specifications design of

26

these microneedles for applications of transdermal drug delivery includes length = 200 μm, inner diameter = 60 μm, outer diameter = 150 μm with 1000 μm center-to-center spacing between microneedles [7]. Simulations were performed for structural and couple multifield analysis [7]. Various voltages and frequencies were examined and compared with flow rates and found that at 100 Volt with frequency of 250 Hz maximum flow rate of 83.99 uL / min was achieved, concluding that higher flow rate is achievable at the lower voltages [7].

Yu-Tang Chen et al [61, 5], design and fabricated "V" groove shaped polymer microneedles and silicon microneedle with the length of 236 μm and 350 μm respectively [61, 5]. Both different material based microneedles were fabricated by two separate techniques, polymer microneedles were formed with turning model technique along with a major material SU-8 2050 and silicon microneedles were shaped with wet etching technology along with the undercut and anisotropic etching[61, 5]. The fabricated microneedles were then tested on the artificial skin and resulted in better performance after invivo into the skin [61, 5].

M.W. Ashraf et al [53], conducted a detailed study and presented the transdermal drug delivery system formed by piezoelectrically actuated microfluid device and fluid reservoir along with silicon out of plane hollow microneedles for the treatment of cardiovascular disorders [53]. The fabricated hollow microneedles have dimension with length = 200 μm, inner diameter = 60 μm, outer diameter = 150 μm and center to center spacing of 1000 μm [53]. Deep reactive ion etching (DRIE) which is followed by inductively coupled plasma (ICP) etching technology were used for the fabrication of these hollow out of plane microneedles with fluid reservoir [53]. The system devices in this study achieved a maximμm flow of 83.99 μm / min with a deflection of 16.48 μm which concluded that piezoelectrically actuated devices do not have maximum flow rate at maximum membrane deflection [53]. The authors reveal that this system is quite helpful for the treatment of hemodynamic dysfunctions [53].

Seung-Joon Paik et al [62], demonstrated the fabrication and design of Transdermal Drug Delivery (TDD) system which is composed of drug reservoir with integration of dissolvable polymer pyramidal tipped microneedle arrays as shown in figure 12 [62]. The microneedles shafts were shaped with process of photolithography while water soluble dissolvable tips of microneedle arrays were fabricated by polydimethylsiloxane (PDMS) molded process and these tips were effectively transferred into agarose gel filled microtubes [62]. Mechanical tests for dissovable tips microneedle array were also performed and these tests revealed successful results after the penetration tests [62]. The fabricated microneedles were 711 μm long including 244 μm long dissolvable tips with top width of 230 μm and shaft bottom width of 500 μm and 380 μm width of pyramidal tip [62].
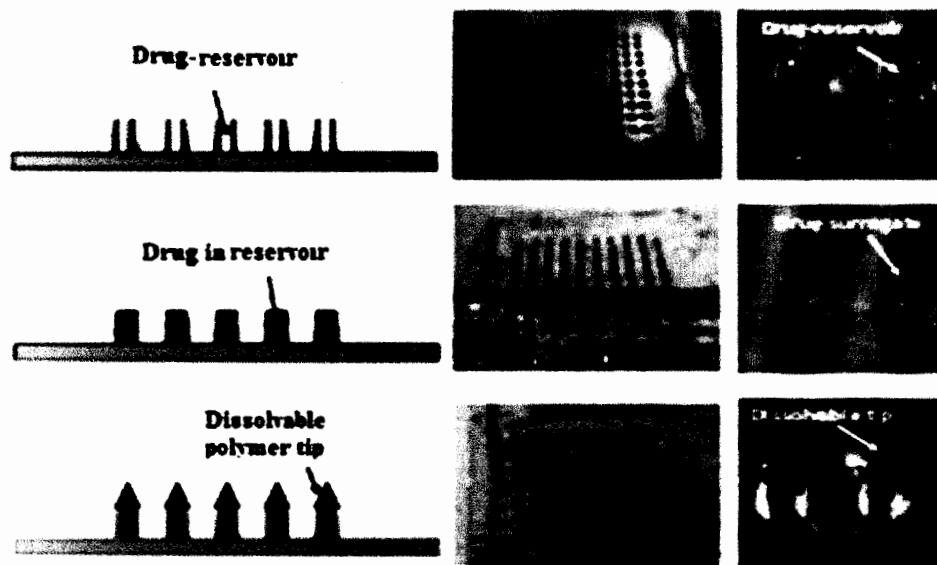
Figure.12 The Fabricated Microneedle Array with Dissolvable Polymer Tip [62]

Peiyu Zhang et al [47], deployed a bi-mask technique for the fabrication of silicon out of plane microneedles with cylindrical body having sharp tip that contains three knife like edges with side openings [47]. These microneedles have array size of 10 x 11 with 200 μm length, inner diameter of 40 μm, three side openings of 28 by 50 μm^2 each sand needle tip with nearly 450 nm [47]. Permeability and fluid flow trials were carried out for effectiveness of microneedle arrays [47].

Ciprian Iliescu et al [63, 64, 9], demonstrated the fabrication of out of plane microneedles array for transdermal drug delivery with biodegradable porous silicon tips by utilizing the techniques of deep reactive ion etching and electrochemical anodization process [63, 64, 9]. Biodegradable porous tips were formed by MeCN/HF/H$_2$O solution of electrochemical anodization process which in turn enhanced its efficiency for TDD [63, 64, 9]. These microneedles are arrayed in matrix of 30 x 30 having a length of 100 μm. Experiments showed effective transport of calcein and BSA drugs through animal skin [63, 64, 9].

Po-Chun Wang et al [65], used the combing UV photolithography and micromolding techniques for the fabrication of hollow polymer pyramidal tip microneedle arrays with base width of 400 μm, 825 μm long height, including 255 μm tall pyramidal tip along with 15 – 25 μm diameter of each tip, hollow lumen with 150 μm diameter arrayed with 10 x 10 matrix [65]. Characterization of these microneedles with fluidic and absorption tests were performed for drug transport efficiency [65].

Puneet Khanna et al [66], depicted to have sharpened tips hollow silicon microneedles shown in figure 13, fabricated with sizes 33 gauge to 36 gauge with their respective inner and outer diameters with the technique of deep reactive ion etching (DRIE) along with involving novel photoresist depletion at the same time in the process [66]. The fabricated sharpened microneedles were experimented on the cadaver skin for penetration tests [66]. The promising results showed that by sharping tips, the invivo skin penetration force was much reduced and there was sustainability in their mechanical strength [66]. For intense sharpened tips the insertion force was reduced to about more than 75 times in magnitude [66]. Many penetration tests were performed from 34 gauge needles with inner diameter and outer diameter of 85 μm and 160 μm respectively along with pitch of 1000 μm with array size of 4 x 4 matrix [66].
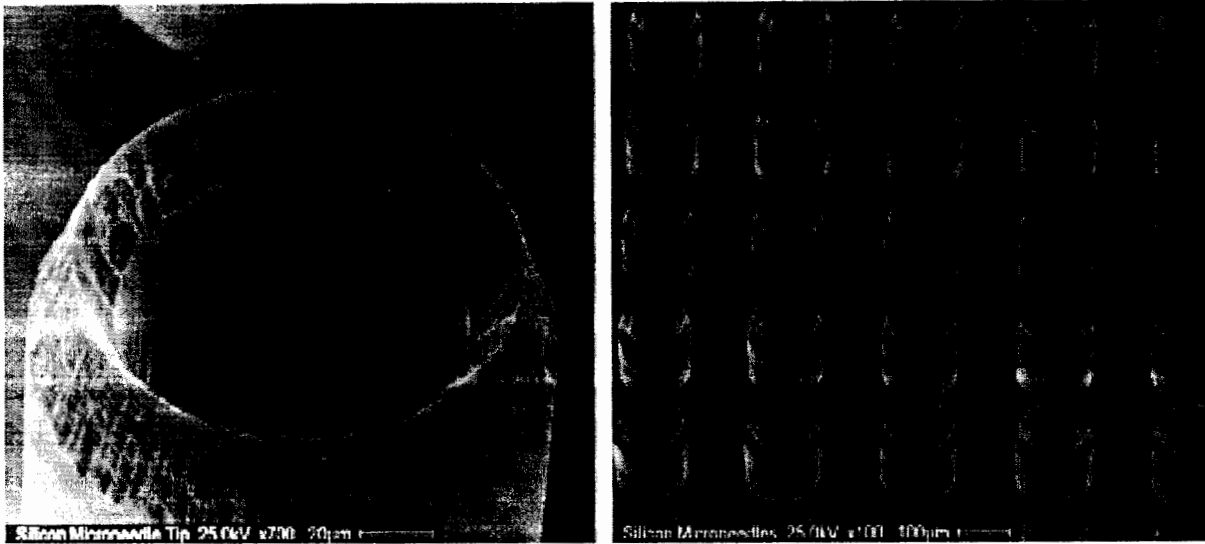
Figure.13 Silicon Microneedles with 'very sharp' Tips [66]

Rajmohan Bhandari et al [2], designed and fabricated high density out of plane microneedle arrays by mask less technique [2]. These microneedle arrays for blood sampling were developed jointly by laser machining, dicing and wet isotropic etching [2]. The presented microneedle arrays composed of array of 10 x 10 matrix with 400 μm pitch and height of 450 μm with lumen diameter of 60 μm [2].

G. Barillaro etal [67], developed silicon chip consisting of hollow silicon dioxide microneedle array with space for fluid reservoir attached independently [67]. These silicon dioxide microneedles were fabricated from electrochemical machining (ECM) technology for applications of transdermal drug delivery and its dimensions comprises of 0.5cm x 0.5cm array size with shaft length of 100 μm, an inner diameter and outer diameter of 4 μm and 6 μm respectively, period of 10 μm and needle density of 1×10^6 needles/cm^2 [67]. The presented ECM technology was said to be a low cost and reliable approach for the mass production of these types of silicon based devices [67].

T. Shibata et al [46], fabricated circler tip shape silicon dioxide microneedle array for chip based system, mainly used for cell surgery manufactured by the combination of photolithography and deep reactive ion etching (DRIE) along with processes of wet oxidation and isotropic etching [46]. These microneedles have length of 77 µm, an inner diameter of 3.5 µm, outer diameter of 5.5 µm and pitch of 26 µm [46]. Silicon dioxide out of plane microneedles has capability to introduce or extract biomolecules in and out of living cells [46]. Experiments for mechanical strength were carried out on an artificial cell and results showed no real damage to the microneedles [46]. Characterization for efficiency and fluid flow were also examined in this study [46].

Jung-Hwan Park et al [68], presented the novel integrated lens technique for fabrication of tapered biodegradable polymer microneedles that can be easily inserted into skin without any damage [68]. The technique is the followed by process of micromolding which creates tapered biodegradable polymer microneedles with variety of dimensions [68]. Different experiments for mechanical and insertion tests were investigated on porcine skin and on human tissue with different length of microneedles ranging from 350 µm to 1500 µm and found that the experimental results are quiet comparable with the theoretical analysis [68]. The qualitative assessments showed that the properties of fabricated microneedles were adequate for the transdermal drug delivery [68].

Sangchae Kim et al [69], studied the design and fabrication of various dimensions and shapes of silicon dioxide out of plane hollow microneedle arrays by utilizing the silicon bulk micromachining technique with deep reactive ion etching (DRIE) approach [69]. These transdermal applications microneedle arrays were then characterized for mechanical and insertion procedures with penetration of stratum corneum and whole skin, the reliability measurements quantified no fractures to microneedles during insertion which ultimately shown the silicon dioxide microneedle arrays robustness [69].

Boris Stoeber et al [8], fabricated painless symmetric and point needles with sharp tips out of plane hollow silicon microneedle arrays for drug delivery having 200 μm long microneedle shaft with 40 μm diameter of channel along with a wide base and 750 μm center to center spacing between positioned with array of 8 needles [8]. These two types of microneedle arrays were fabricated by bulk micromaching technique with joint combination of deep reactive ion etching (DRIE) and isotropic etching process [8]. The symmetric needles were fabricated when center of channel was in contact with mask center [8]. Liquid injection test for these point microneedles were performed by incorporated silicon plate to the end of plastic syringe and injected into deep 100 μm skinless chicken with fluorescent marker Lucifer Yellow by applying different lateral forces [8]. Liquid flow characterization was carried out and individual needle is modeled with modified Bernoulli equation for fluid flow through microneedles and concluded that the mean values were have 2% difference between theoretical and experimental results [8]. In additional the authors also concluded that for microneedles lumens, the Bernoulli equation was a good model for fluid flow [8].

Md Shofiqul Islam et al [70], employed an optimum process for fabrication of silicon mironeedles with high aspect ratios for biomedical applications [70]. Simulations were performed on the SILVCO process simulator ATHENA for fabrication of microneedles by varies parameters including etch time, etch rate and isotropy coefficient etc [70]. Reactive ion etching (RIE), wet etching and plasma etching techniques were used for fabrication of these microneedles with different dimensions and results were compared among these three techniques [70]. Characterization for fluid flow and mechanical strength were performed and only RIE technique resulted in biocompatibility of these microneedles for biomedical applications [70]. Comparison results among above three techniques revealed that Reactive Ion Etching (RIE) was the only technique from where optimized shape microneedles could be fabricated with damage profiles [70].

Md. Nurul Abser et al [71], successfully designed and fabricated circular and prismatic shaped "out of plane" beveled tips mironeedles for drug delivery to the posterior part of the human eye [71]. These microneedles were fabricated as shown in figure 14 by using isotropic RIE technique and etchant SF_6/O_2 [71]. Simulations for microneedles fabrication process were performed on SILVACO process simulator ATHENA [60]. Processes for fabrication were defined by machine parameters of ATHENA with heights ranging from 450 μm to 700 μm and base widths from 10 μm to 15 μm [71]. Tests of mechanical properties were carried out for these microneedles and the analysis showed that buckling and bending forces were much greater indicating that the fabricated microneedles without any fracture could deliver drug to the human eye and withstand all the exerted pressures [71]. Figure 15 shows 450 μm long beveled tip silicon microneedle [71].
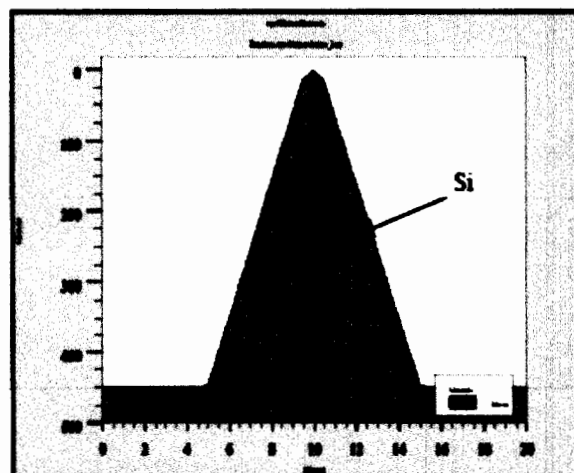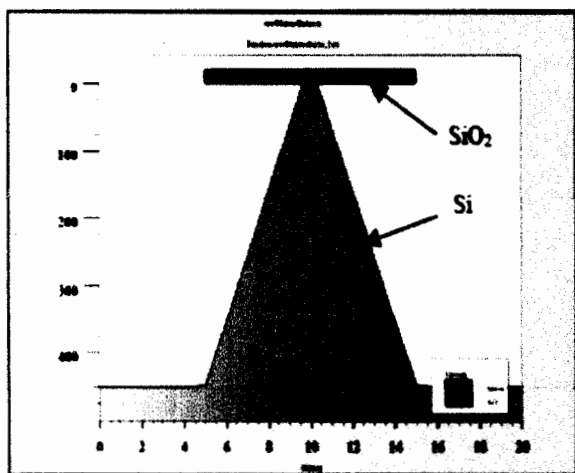
Figure.14 Microneedle with Complete RIE Process [71] Figure.15 450μm long Beveled Tip Microneedle [71]

4.2 Summary of Literature Review

The table 7 illustrates the summary of the literature review with microneedles structure, shapes, materials, Fabrication techniques and their industrial applications.

Table.7   Summary of the Literature Review

MICRONEEDLES STRUCTURE / SHAPES	MICRONEEDLES DIMENSIONS / ARRAY SIZE	MATERIAL	FABRICATION TECHNIQUES	APPLICATIONS	REFERENCES
Hollow, out of plane / sharp beveled tips / side open lumen	Length = 1mm Lumen diameter =150 µm Array size= 6 x 6	Polymer SU - 8	UV photolithography/ micromolding	Transdermal drug delivery	Po-Chun Wang et al. [59]
Out of plane / conical shape / arrow head tips	Length = 800 µm Neck diameter = 240 µm Array size=10x 10	Mixture of polymer PVA, PVP and water	Micromolding /direct drawing	Transdermal drug delivery	Jooncheol Kim et al. [6]
Hollow, out of plane / Cylindrical shape	Length = 200 µm Inner diameter = 60 µm Outer diameter = 150 µm Array size= 5 x 5	Silicon	Inductively coupled plasma (ICP) etching	Transdermal drug delivery	Muhammad Waseem Ashraf et al. [48]
·Hollow, out of palne / cylindrical shape	Length = 1540 µm Inner diameter = 100 µm Wall thichness = 15 µm	Polymer SU - 8	Deep reactive ion etching (DRIE)	Transdermal drug delivery / blood extraction	Buddhadev Paul Chaudhri et al. [60]
Hollow / cylindrical shape / tapered tip	Length = 200 µm Inner diameter =60 µm Outer diameter = 150 µm Center to center spacing=1000 µm	Silicon	DRIE / ICP etching	Transdermal drug delivery	D.W. Bodhale et al. [7]
Out of plane / V groove shape	Length = 236 µm, 350 µm	SU - 8 / Silicon	Turning model technique / wet etching KOH etching	Biomedicine technology	Yu-Tang Chen et al. [61] Chin-Chun Hsu et al. [5]
Hollow,out of plane / cylindrical shape	Length = 200 µm Inner diameter = 60 µm Outer diameter = 150 µm Pitch = 1000 µm Array size= 5 x 5	Silicon	Inductively coupled plasma (ICP) etching	Transdermal drug delivery (for treatment of cardiovascular disorders)	M.W. Ashraf et al. [53]
Out of plane / pyramidal dissolvable tips	Total Length = 711 µm Length of dissolvable tips = 244 µm Tips top width =	Polymer SU-8 for pillars and	Photolithography / molding process	Transdermal drug delivery	Seung-Joon Paik et al. [62]

	230 μm Shaft bottom width = 500 μm Width of tip = 380 μm	water soluble polymer for sharp tips			
Out of plane / cylindrical body / sharp tips with three knife like edges / side opens	Length = 200 μm Inner diameter = 40 μm Side openings = three 28 by 50 μm^2 each. Needle tip = 450 nm Array size=10 x11	Silicon	Bi mask technique	Transdermal drug delivery	Peiyu Zhang et al. [47]
Out of plane / biodegradable sharp tips	Length = 100 μm Array size = 30 x 30	Silicon / porous silicon for tips	DRIE / Electrochemical etching	Transdermal drug delivery	Ciprian Iliescu et al. [63] Bangtao Chen et al. [9] Bangtao Chen et al. [64]
Hollow, out of plane / pyramidal tip	Length = 825 μm includes 255 μm tall pyramidal tip. Base width = 400 μm. Inner diameter = 150 μm. array size=10 x 10	Polymer SU-8	UV photolithograpy / Micromolding process	Transdermal drug delivery	Po-Chun Wang et al. [65]
Hollow, out of plane / cylindrical / sharp tip	Length = 33 gauge to 36 gauge. Inner diameter = 100 μm, 85 μm, 65 μm, 30 μm. Outer diameter = 200 μm, 160 μm, 130 μm, 100 μm. Pitch = 1000 μm Array size =4 x 4	Silicon	DRIE involve photoresist depletion	Transdermal drug delivery	Puneet Khanna et al. [66]

35

Hollow, out of plane	Length = 450 µm Hole diameter = 60 µm Pitch = 400 µm Array size=10x10	Silicon	Mask less technique	Blood sampling	Rajmohan Bhandari et al. [2]
Hollow	Length = 100 µm Inner diameter = 4 µm Outer diameter = 6 µm Period = 10 µm Needle density =1x10^6 needles/cm^2	Silicon dioxide (SiO$_2$)	Electrochemical machining (ECM) technology	Transdermal drug delivery	G. Barillaro et al. [67]
Hollow, out of plane / circler tip shape	Length = 77 µm Inner diameter = 3.5 µm Outer diameter = 5.5 µm Pitch = 26 µm	Silicon dioxide (SiO$_2$)	Photolithograpy / DRIE	Cell surgery	T. Shibata et al. [46]
Out of plane / Tapered tip shape	**a) Dimensions produced from lens technique** Lengths = 980 µm, 750 µm ,1070 µm Tip diameters= 26 µm, 150 µm, 120 µm Center to center spacing = 400 µm and 800 µm. Array size=20x10 **2. Dimensions of biodegradable polmers microneedles produced from micromolding.** Length = 1500 µm, 75 µm, 400 µm Base diameter= 250 µm, 150 µm, 100 µm Tip diameter= 10 µm, 5 µm, 30 µm Array size = 200	Polymers SU-8 PGA PLA PLGA	Integrated lens technique / Micromolding	Transdermal drug delivery	Jung-Hwan Park et al. [68]

Design	Dimensions	Material	Fabrication	Application	Reference
Hollow, out of plane / Square shape / circular shape	**a)** Length = 100 μm Width = 40 μm Pitch = 150 μm Array size=25x25 **b)** Length = 105 μm Width = 60 μm Pitch = 150 μm Array size=25x25	Silicon dioxide (SiO$_2$	Bulk micromaching	Transdermal applications	Sangchae Kim et al. [69]
Hollow, out of plane / Symmetric shape needle / pointed shape needle / sharp tips	Length = 200 μm Channel diameter =40 μm Wide base = 425 μm Array size = 8 needles Distance between needles = 750 μm	Single crystal silicon	DRIE / Isotropic etching	Epidermal drug delivery	Boris Stoeber et al. [8]
Hollow, out of plane / optimized shape with tapered side wall / circular ball shape / convex with flat tip shape.	**a)** Length = 145 μm Base width = 5 μm Channel width =1 μm Tapered side wall=2 μm Needle tips with sidewalls= 0.5 μm Needle to needle distance < 600 μm Array size=6x6 **b)** Length=68 μm Base width= 12 μm Sidewall =1.81μm Needle to needle distance < 600 μm Array size=6x6	Silicon	RIE / Wet etch / Plasma etch	Biomedical applications	Md Shofiqul Islam et al. [70]
Solid, out of plane / prismatic and circular shape/ beveled tips	Length = 450 μm, 550 μm, 600 μm, 700 μm Base width = 10 μm, 12 μm, 15 μm, 15 μm	Silicon	Isotropic RIE technique / etchant SF$_6$/0$_2$	Drug delivery to human eye	Md. Nurul Abser et al. [71]

MODELING EXPERIMENTS -
HOLLOW MICRONEEDLE FLUIDIC ANALYSIS

It is very significant to develop appropriate numerical model for microneedles with the characteristics of fluid flow and to account for "lumen dimensions" as the liquid drugs invivo into the skin through these arrays of microneedle. Therefore; mathematical models are developed in this chapter to evaluate and comprehend the working performance of microneedle arrays theoretically.

5.1 Bernoulli Equation Mechanics

One of the most valuable equations in the fluid mechanics is the Bernoulli equation (BE). BE is an expression for the statement of conservation of energy along a stream line therefore the summation of overall energy in a passive fluid stream at any point must be constant [72, 73]. Bernoulli equation forms relationship among velocity, pressure and elevation in a flow field [74].

The Bernoulli equation consists of three different energies that are [75].

(a) Flow energy $= P\,Q$, where, P = Pressure and Q = Volume flow rate;

(b) Potential energy $= mgZ$, where m = mass, g = gravity and Z = Altitude;

(c) Kinetic energy $= \dfrac{mV^2}{2}$, where m = mass and V = mean velocity;

By summing all above energies the total energy must be equal to:

$$E_T = P_1Q_1 + mgZ_1 + \frac{mV_1^2}{2} = P_2Q_2 + mgZ_2 + \frac{mV_2^2}{2} \tag{1}$$

Divide equation (1) by mass m gives:

$$E_T = \frac{P_1}{\rho_1} + gZ_1 + \frac{V_1^2}{2} = \frac{P_2}{\rho_2} + gZ_2 + \frac{V_2^2}{2} \tag{2}$$

Now again divide equation (2) by g gives energy form per unit weight:

$$\frac{E_T}{mg} = \frac{P_1}{\rho_1 g} + Z_1 + \frac{V_1^2}{2g} = \frac{P_2}{\rho_2 g} + Z_2 + \frac{V_2^2}{2g} \tag{3}$$

The density is same at both points for the liquids for equation (3) therefore the total pressure is:

$$P_T = P_1 + \rho g Z_1 + \frac{\rho V_1^2}{2} = P_2 + \rho g Z_2 + \frac{\rho V_2^2}{2} \tag{4}$$

The friction energy losses cause an increase in the temperature and hence rise in the internal energy. With the equilibrium lost, an additional term is added in equation (4) to sustain the balance of the equation. This additional term is referred as "pressure loss" P_L. The equation in form of pressure is as follows:

$$P_1 + \rho g Z_1 + \frac{\rho V_1^2}{2} = P_2 + \rho g Z_2 + \frac{\rho V_2^2}{2} + P_L \tag{5}$$

Besides energy loss the fluid total energy is also no longer constant. So Bernoulli equation is terms of pressure loss is also written as.

$$P_L = P_1 - P_2 + \rho g Z_1 - \rho g Z_2 + \frac{\rho V_1^2}{2} - \frac{\rho V_2^2}{2} \tag{6}$$

$$P_L = P_1 - P_2 + \rho g (Z_1 - Z_2) + \rho \left(\frac{V_1^2 - V_2^2}{2} \right) \tag{7}$$

In equation (7), P_1 is inlet pressure, P_2 is outlet pressure, v_1 is inlet velocity, v_2 is outlet velocity, Z_1 is inlet height, Z_2 is outlet height and ρ is fluid density [74].

5.2 Equation of Motion for Flow in a Microchannel

The flow in a microchannel is model with Darcy-Wesibach equation [76] which narrates the "average velocity of a given length of pipe with a pressure loss due to friction" [76] i – e

$$P_1 - P_2 = \rho \frac{V^2}{2g} \frac{fL}{D}$$ (8)

The pressure loss in the above equation is given as the product of kinetic energy of flow and friction term which is $\frac{v^2}{2g}$ and $\frac{fL}{D}$ respectively, and it is independent of microchannel cross section. The equation (8) is used with Bernoulli equation to model the flow in a microchannel i – e

$$P_1 - P_2 + \rho g(Z_1 - Z_2) + \rho \left(\frac{V_1^2 - V_2^2}{2} \right) = \rho \frac{V^2}{2g} \frac{fL}{D}$$ (9)

This expression explains that when an "appropriate" diameter is used, it can be applied to any cross section.

5.3 Minor Pressure Losses

Minor losses are the pressure losses encountered in a fitting or in piping system via fluid during the flow [74]. When the fluid flows through, the area might be abruptly changing due to this flow which in turns encounters a pressure loss. This pressure loss is mathematically treated by applying a loss factor "K" to each fitting which is then expressed as a multiple of kinetic energy of the flow [74].

$$P_1 - P_2 = \sum K \frac{\rho V^2}{2g}$$ (10)

Where $\sum K$ is the minor losses encounter during travelling via fluid particle [74].

By combing the Bernoulli equation with equation (8), given an expression encompassing the effect of friction and minor pressure losses equation (10), the equation results in [7,8,14,43,48,53,72,74],:

$$P_1 - P_2 + \rho g(Z_1 - Z_2) + \rho \left(\frac{V_1^2 - V_2^2}{2}\right) = \rho \frac{V^2}{2} \frac{fL}{D} + \Sigma K \frac{\rho V^2}{2} \qquad (11)$$

This is called "Modified Bernoulli Equation" [7,8,14,43,48,53,72,74], with neglecting gravitational forces "g".

$$P_1 - P_2 + \rho g(Z_1 - Z_2) + \rho \left(\frac{V_1^2 - V_2^2}{2}\right) = \rho \frac{V^2}{2g} \frac{fL}{D} + \Sigma K \frac{\rho V^2}{2g} \qquad (12)$$

When the value and contribution of 'g' is not neglected, we come up with a solution i – e equation (12) above which is now labeled as the "Extended Modified Bernoulli Equation".

5.4 Reynolds Number

The Reynolds number defined as follows, used in later pressure drop analysis indicates the type of flow [7, 53].

$$Re = \frac{\rho V D}{\mu} \qquad (13)$$

Where ρ, μ and V represent density, viscosity and *velocity* of the fluid respectively and D is the diameter of lumen. The flow is laminar when Re is less than 2100, otherwise the flow is regarded as turbulent [7, 53]. Fortunately, fluid flow follows laminar regime in most of small scale device applications such as microneedle [14].

5.5 Flow Characteristics through Microneedle Arrays

5.5.1 Analysis for Pressure Drop

Properties such as microneedle geometry, viscosity of fluid, microneedle density and flow rate are mainly acquired by the pressure drop in order to allow the flow of fluid through microneedles [53]. There are two approaches for analysis of pressure drop for an individual needle:

(a) Modified Bernoulli equation, where the gravitational forces are ignored in calculations and analysis reported in literature such as reference [8].

(b) Desired Extended modified Bernoulli equation, where the gravitational forces are not ignored in calculations and analysis which are reported in this thesis.

5.5.1.1 Pressure Drop Analysis From Modified Bernoulli Equation

An individual microneedle has been modeled using water as a "model liquid" as shown in figure 16 with Modified Bernoulli Equation which is used to depict fluid flow through microneedle [8]. In case of considered needle, the channel with a "constant" cross section area, equation (11) can be further reduced.
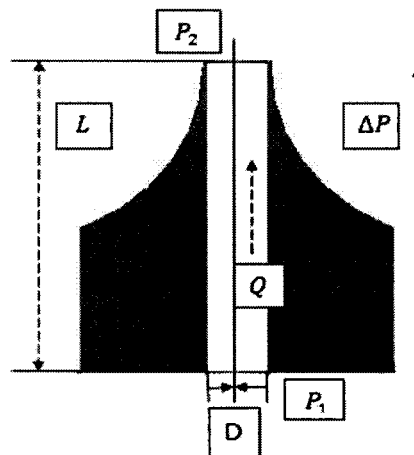
Figure.16 Characteristics of Liquid Flow Through Microneedle

First considering Darcy-Wesibach equation from equation (11), we have

$$\Delta P = \rho \, \frac{V^2}{2} \, \frac{fL}{D} \qquad (14)$$

Here $V = \frac{Q}{A}$ and $f = \frac{64}{Re}$

$$\Delta P = \frac{\rho}{2} \, \frac{Q^2}{A^2} \, \frac{64}{Re} \, \frac{L}{D} \qquad (15)$$

Here $A = \frac{\pi D^2}{4}$ and $Re = \frac{\rho VD}{\mu}$

$$\Delta P = \frac{\rho}{2} \, \frac{Q^2}{\left(\frac{\pi D^2}{4}\right)^2} \, \frac{64}{\frac{\rho VD}{\mu}} \, \frac{L}{D} \qquad (16)$$

On further simplifying

$$\Delta P = \frac{2Q}{\pi D^4} \, 64\mu \, L \qquad (17)$$

Rearranging the equation we have

$$\Delta P = \mu \, \frac{128}{\pi} \, \frac{QL}{D^4} \qquad (18)$$

The above equation shows that for laminar flow the Darcy-Wesibach equation is similar to Hagen Poiseuille relation [7,53] which is the equation for flow rate "Q" in terms of pressure drop (ΔP). This equation also tells that inside a circular tube the viscous shear force of Poiseuille flow induced the pressure drop [77].

Secondly, now considering the minor pressure losses equation from equation (11), we have:

$$\Delta P = \sum K \ \frac{\rho V^2}{2} \tag{19}$$

$$\Delta P = \frac{\sum K}{2} \ \rho V^2 \tag{20}$$

Here $V = \frac{Q}{A}$

$$\Delta P = \frac{\sum K}{2} \ \rho \frac{Q^2}{A^2} \tag{21}$$

Here $A = \pi D^2 / 4$

$$\Delta P = \frac{\sum K}{2} \ \rho \ \frac{Q^2}{\left(\frac{\pi D^2}{4}\right)^2} \tag{22}$$

$$\Delta P = \sum K \ \rho \ \frac{Q^2 \ 8}{\pi^2 \ D^4} \tag{23}$$

Rearranging above equation:

44

$$\Delta P = \rho \; \frac{8 \sum K}{\pi^2} \; \frac{Q^2}{D^4} \tag{24}$$

$$\Delta P = \rho \; \frac{8(K_1 + K_2)}{\pi^2} \; \frac{Q^2}{D^4} \tag{25}$$

The above equation corresponds to inertia effects along with the minor losses K_1 & K_2 at the entrance and exit of the needle respectively [43].

By combing the equation (18) and equation (25) the modified Bernoulli equation reduces to:

$$\Delta P = \mu \; \frac{128}{\pi} \; \frac{QL}{D^4} + \rho \; \frac{8 (K_1 + K_2)}{\pi^2} \; \frac{Q^2}{D^4} \tag{26}$$

The above equation (26) illustrates that the contribution from the gravitational force 'g' are neglected. In the above calculations Gravitational forces were not considered because in previous studies it was assumed that at the time of experiments of flow, they might be negligible being relatively small [8]. This, however, is tested in our studies conducted during the design and modeling of such microneedle devices.

5.5.1.2 Pressure Drop analysis from Extended Modified Bernoulli Equation

Just like in section 5.5.1.2, an individual needle also has been modeled with Extended Modified Bernoulli Equation which is also mainly proposed to describe geometric effects under the influence of gravitational forces for fluid flow for applications in biomedical systems. In case of considered needle the channel with a constant cross section area, equation (12) can be reduced further.

First considering Darcy-Wesibach equation from equation (12), we have:

$$\Delta P = \rho \, \frac{V^2}{2\,g} \frac{fL}{D} \tag{27}$$

$$\text{Here } V = \frac{Q}{A} \text{and } f = \frac{64}{Re}$$

$$\Delta P = \frac{\rho}{2\,g} \frac{Q^2}{A^2} \frac{64}{Re} \frac{L}{D} \tag{28}$$

$$\text{Here A} = \frac{\pi D^2}{4} \text{ and Re} = \frac{\rho V D}{\mu}$$

$$\Delta P = \frac{\rho}{2\,g} \frac{Q^2}{\left(\frac{\pi D^2}{4}\right)^2} \frac{64}{\frac{\rho V D}{\mu}} \frac{L}{D} \tag{29}$$

On further simplifying:

$$\Delta P = \frac{1}{g} \frac{2Q}{\pi D^4} \, 64\mu \, L \tag{30}$$

Rearranging the above equation:

$$\Delta P = \mu \; \frac{128}{\pi \; g} \; \frac{QL}{D^4} \tag{31}$$

This equation tells about the influence of gravitational forces 'g' along with the pressure drop inside a circular duct of Poiseuille flow due to the viscous shearforce.

Second, now considering minor pressure losses equation from equation (12), we have:

$$\Delta P = \Sigma K \; \frac{\rho V^2}{2 \; g} \tag{32}$$

$$\Delta P = \frac{\Sigma K}{2 \; g} \; \rho V^2 \tag{33}$$

Here V = Q / A

$$\Delta P = \frac{\Sigma K}{2 \; g} \; \rho \frac{Q^2}{A^2} \tag{34}$$

Here A = π D^2 / 4

$$\Delta P = \frac{\Sigma K}{2 \; g} \; \rho \; \frac{Q^2}{\left(\frac{\pi D^2}{4}\right)^2} \tag{35}$$

On further simplifying:

$$\Delta P = \frac{\Sigma K}{g} \; \rho \; \frac{Q^2 \; 8}{\pi^2 \; D^4} \tag{36}$$

Rearranging above equation:

$$\Delta P = \rho \; \frac{8 \sum K}{\pi^2 g} \; \frac{Q^2}{D^4} \tag{37}$$

$$\Delta P = \rho \; \frac{8(K_1 + K_2)}{\pi^2 g} \; \frac{Q^2}{D^4} \tag{38}$$

This equation corresponds to inertia effects along with the minor losses K_1 & K_2 at the entrance and exit of the needle respectively [43] under the influence of gravitational forces 'g', which may be of greater importance when using the devices on altitudes.

By combing the equation (31) and equation (38) the extended modified Bernoulli equation reduces to

$$\Delta P = \mu \; \frac{128}{\pi \, g} \; \frac{QL}{D^4} + \rho \; \frac{8 \, (K_1 + K_2)}{\pi^2 \, g} \; \frac{Q^2}{D^4} \tag{39}$$

The above expression illustrates that gravitational forces 'g' should not be neglected but it must be taken into account while doing analysis for pressure drop and flow rate for microneedles, particularly on conditions where application ambient is on altitudes.

5.5.2 Analysis for Microchannel Diameter

Diameter is one the utmost parameter for the design of microneedle because it describes the "channel inner" from where the fluid flows and injected into the skin. This parameter is dealt with full appreciation in our design.

(a) Analysis of microchannel using diameter from pressure drop equation where the gravitational forces "g" are ignored:

$$\Delta P = \mu \; \frac{128}{\pi} \; \frac{QL}{D^4} + \rho \; \frac{8 \, (K_1 + K_2)}{\pi^2} \; \frac{Q^2}{D^4} \tag{40}$$

$$\Delta P = \frac{1}{D^4} \left(\mu \frac{128}{\pi} QL + \rho \frac{8 (K_1 + K_2)}{\pi^2} Q^2 \right) \tag{41}$$

On further simplifying:

$$D = \left(\mu \frac{128}{\pi \Delta P} QL + \rho \frac{8 (K_1 + K_2)}{\pi^2 \Delta P} Q^2 \right)^{0.25} \tag{42}$$

(b) Analysis of microchannel using diameter from pressure drop equation where the gravitational forces are contributed:

$$\Delta P = \mu \frac{128}{\pi g} \frac{QL}{D^4} + \rho \frac{8 (K_1 + K_2)}{\pi^2 g} \frac{Q^2}{D^4} \tag{43}$$

$$\Delta P = \frac{1}{D^4} \left(\mu \frac{128}{\pi g} QL + \rho \frac{8 (K_1 + K_2)}{\pi^2 g} Q^2 \right) \tag{44}$$

On further simplifying:

$$D = \left(\mu \frac{128}{\pi g \Delta P} QL + \rho \frac{8 (K_1 + K_2)}{\pi^2 g \Delta P} Q^2 \right)^{0.25} \tag{45}$$

The summary of the underlying assumption for our design are as follows:

For equations (26), (39), (42) and (45), $f = \frac{64}{Re}$ is the friction factor has been used for laminar flow. Standard macroscopic values for an edged inlet ($K_1= 0.5$) and for an exit ($K_2= 1.0$) were chosen [8, 74] to model the flow characteristics of the $L = 550$ μm long microneedle lumen [8]. $\mu = 1.006e^{-3}$ Pa s and $\rho = 1000$ kg/m^3 were assumed as viscosity and density respectively [8, 74] and g = 9.81 m/s^2 is the gravitational force (subject to change on standard calculations for altitudes).

DESIGN EXPERMENTS I –

DESIGN AND FABRICATION PROCESSES OF MICRONEEDLES

6.1 Experimental tool: MEMS PRO

MEMS Pro is a computer aided design tool provided by the SOFTMEMS Company that relatively utilized for the scalable design, modeling and analysis of Micro Electro Mechanical Systems (MEMS) [78]. The MEMS Pro tool suite as shown in figure.17 consists of Schematic Capture (S-Edit), Simulator (T-Spice Pro), Layout Editor (L-Edit), Layout vs Schematic (LVS), External Model Generator, ANSYS and MemsModulers [78, 79]. These tools offer advancement for the multiple flows among various design and circuit engineers, exchange valuable information between different levels including structural, behavioral , description and physical levels [78].
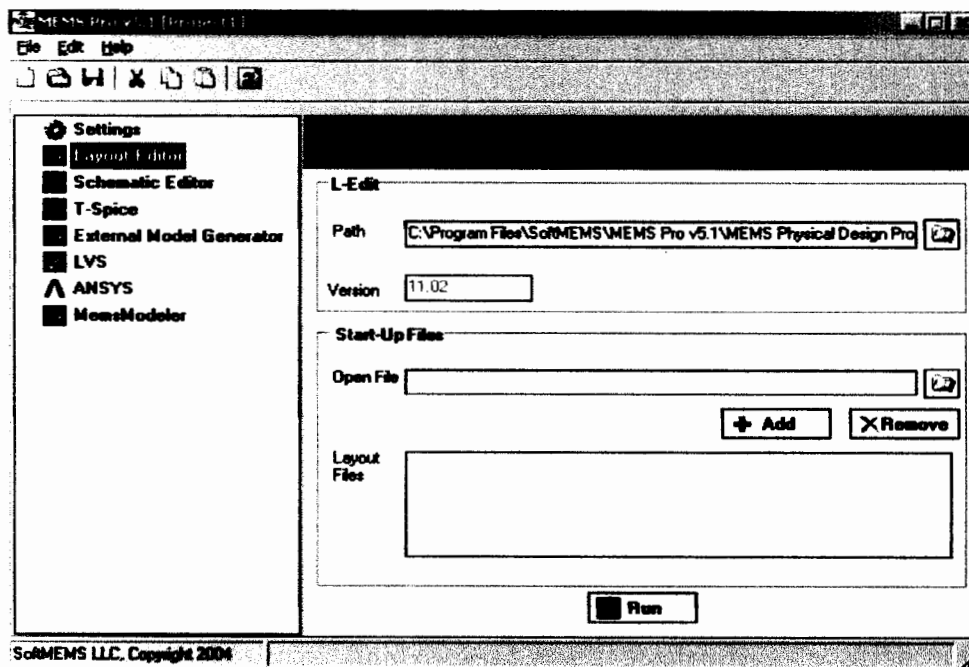
Figure.17 MEMS Pro Tool Suite

6.2 MEMS PRO Key Features

Following are the key features of MEMS Pro design tool [78, 79].

> MEMS Pro incorporates with the capability of schematic capture and behavioral simulation;

> It provides with the facility of MEMS Moduler tool to create behavioral model automatically from 3D and Finite Element Analysis data;

> A library browser is provided to invoke the MEMS optical, fluidic, mechanical, thermal and electrostatic devices layouts;

> MEMS Pro tool provides the facility to view the devices in 3D;

> This design tool provides with capability of design verification tool to debug the errors in MEMS layout design;

> Provides Layout Editor for graphical and physical design with custom mask editor environment having MEMS related capabilities as shown in figure 18;
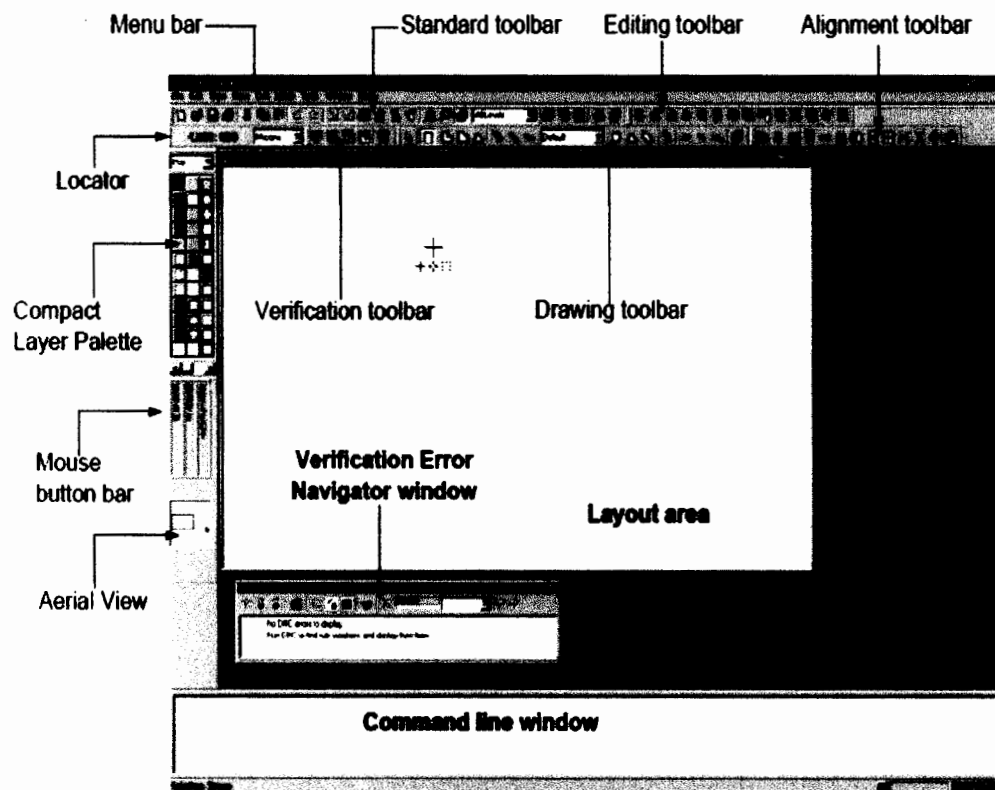
Figure.18 Layout Editor

6.3 Design Consideration for Microneedles

The properties of the needles are generally reflected by the structure of microneedles [47, 54]. The primary considerations for our proposed design of microneedles are:

(a) That during the insertion into skin they must not break or bend. This demands a needle with sharp or pointed tip along with a wide base must be taken into account.

(b) That during the injection period, there are some lateral forces that tends to act on the microneedles, which in turn produce bending moments on the needle body. This demands that the microneedles must have such good design that they withstand with all certain forces.

(c) That one needs to organize the microneedles in the form of arrays because by designing them in arrays the fluid obtained would be in large volume and also be able to have a penetration onto the skin over a large distributed area [8, 54]. As the needle penetration efficiency may be decreased due to high density of microneedles, special care must be taken when needles are arrayed. For successful resulted microneedle, it must have pointed tips, hollow and out of plane shape.

6.4 Fabrication Processes Steps for Microneedles

In order to sketch out the 200 μm long hollow out of plane symmetric microneedle array for biomedical applications, simulations for fabrication process on process simulator MEMS Pro were executed and illustrated in the following steps:

STEP 1

The design process started with initial substrate of silicon wafer with 550 μm thickness shown in figure 19, having <100> orientation and polished on top and bottom side.
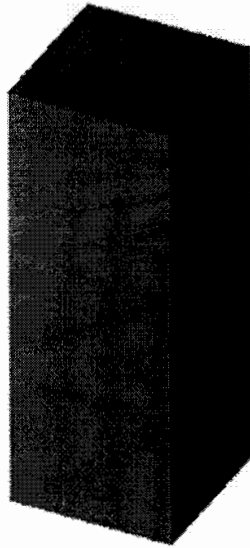
Table.8 Parameters of Initial Substarte

PARAMETERS
Material: Silicon
Thickness: 550 μm
Orientation: <100>

Figure.19 Silicon wafer

STEP 2

The second step is to deposit mask material on the top (surface side) and bottom (bulk side) of the silicon wafer shown in figure 20 and for this purpose 6 μm thickness of silicon dioxide (SiO₂) is deposit by applying a process of Low Pressure Chemical Vapor Deposition (LPCVD).

Figure.20 Deposition of SiO$_2$

Table.9 Parameters of Deposition of SiO$_2$

Material: Silicon dioxide
Thickness: 6 µm
Deposit type: Conformal
Face: Top and Bottom

STEP 3

Photoresist is then deployed on the bottom side of the wafer and by applying photolithography, process pattern was transferred on the oxide layer (SiO$_2$) for the hole of 40 µm in diameter shown in figure 21.

Figure.21 Backside Etching of SiO$_2$
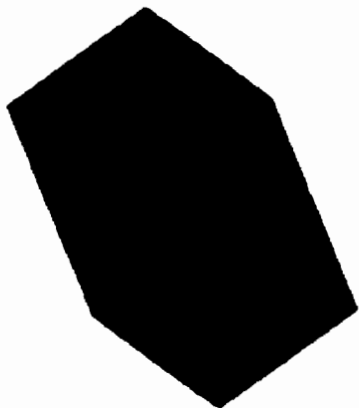
Table.10 Parameters of Backside Etching of SiO$_2$

Photolithography to process the pattern on oxide layer (SiO$_2$)
Etch type: Wet aniso
Depth: 40 µm
Face: Bottom

STEP 4

The anisotropic etching which accomplish by Deep Reactive Ion etching (DRIE) is applied to form the needle channels deep down the silicon substrate to a depth of 556 μm from bottom side stopping close to the top oxide layer as shown in figure 22.

Table.11 Parameters of DRIE for Needle Channel

Channel formation by DRIE
Etch type: Dry
Depth: 556 μm to 0 μm
Face: Bottom

(a)   (b)
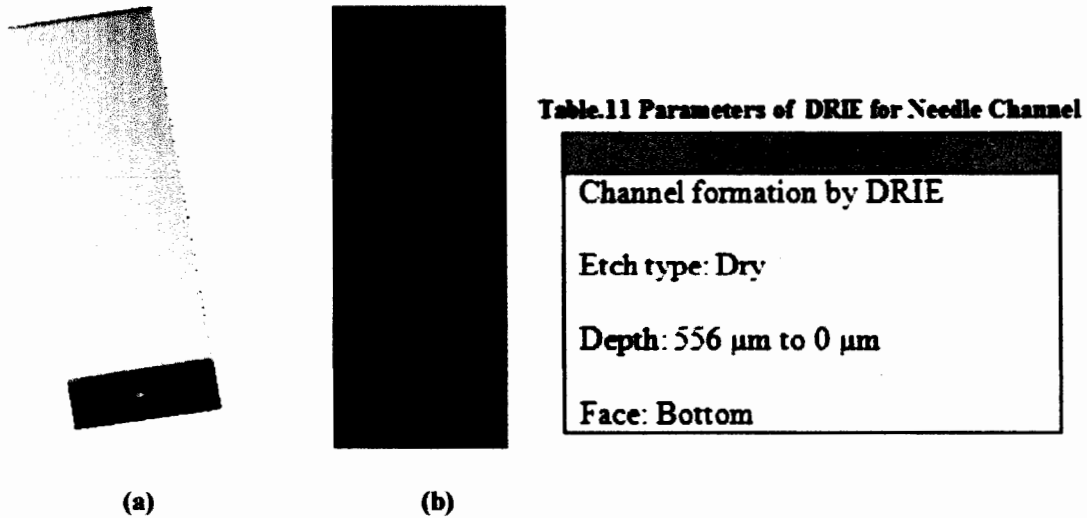
Figure.22 (a) DRIE for Needle Channel (b) Inner Side Strcture after DRIE

STEP 5

4 μm thickness of silicon nitride by applying a process of LPCVD is deposited on the top and bottom along with the channels shown in figure 23 which will act as a protector during the next steps of etching including isotropic etching of silicon.

STEP 7

Now to craft the outer shape of the needle, isotropic underetched is performed as used in previous studies [8] shown in figure 25. The isotropic undercut parameter is primarily utilized to optimize the etching of silicon beneath the circular masks horizontally. Here the silicon nitride plays its critical role and protects the side walls of channels. The obtained outer shape of the needle has a 200µm long shaft with a wide base.
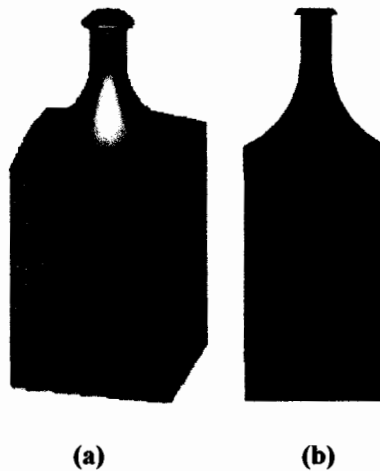
Table.14 Parameters of Isotropic Etching for Needle Shaft

Definition of isotropic undercut ⇩ Attainment of the outer shape of the needle with 200 µm long shaft
Etching type: Wet iso
Face: Top

(a)   (b)

Figure.25 (a) Isotropic Etching for Needle Shaft (b) Inner Side Structure after Isotropic Etching

STEP 8

In the last step the remaining silicon dioxide and silicon nitride are stripped resulting in a final structure of microneedle as shown in figure 26.
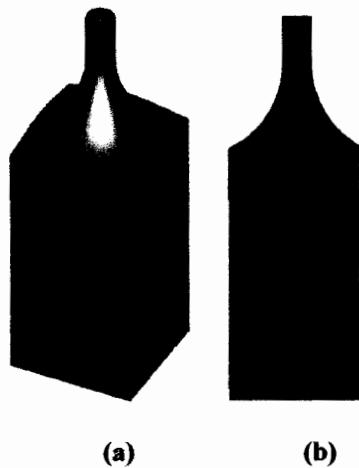
Table.15 Parameters of Removal of SiO_2 and Si_3N_4

Stripping ⇩ Removal of remnant oxide and nitride films
Etching type: Sacrificial

(a)   (b)

Figure.26 (a) Removal of SiO_2 and Si_3N_4 (b) Inner Side Structure after removal of SiO_2 and Si_3N_4
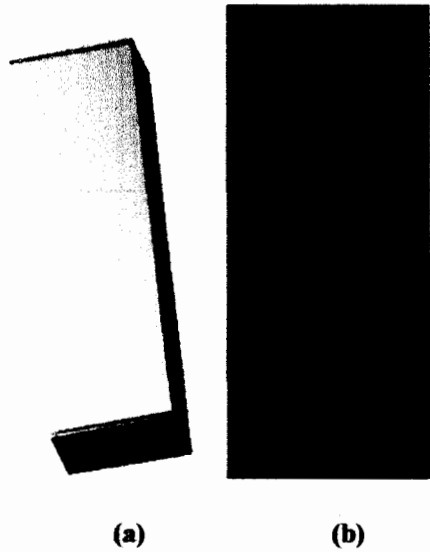
Table.12 Parameters of Deposition of Si₃N₄

Deposition of Si₃N₄ on the top and bottom along with channels
Deposition type: Conformal
Thickness: 4 µm

Figure.23 (a) Deposition of Si₃N₄ (b) Inner Side Strcture after Deposition

STEP 6

On the front side of the wafer photoresist was deployed and circular pattern was transferred by applying photolithography process on the silicon dioxide and silicon nitride masks shown in figure 24 which could be utilize in the next step to create the needle shaft.
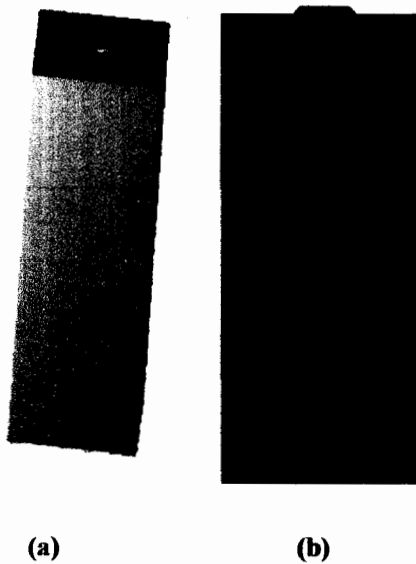
Table.13 Parameters of Pattern Transfer for Front Side

Photolithography to deploy circular pattern
Etching type: Wet aniso
Depth: 10 µm
Masks: SiO₂ and Si₃N₄
Face: Top

Figure.24 (a) Pattern Transfer for Front Side (b) Inner Side Structure after Pattern Transfer

6.5 Summary of the Fabrication Processes Steps for Microneedles

Figure.27 Summarize the fabrication processes steps for hollow out of plane microneedles.

(a)   (b)

(c)   (d)

(e)   (f)

(g)   (h)
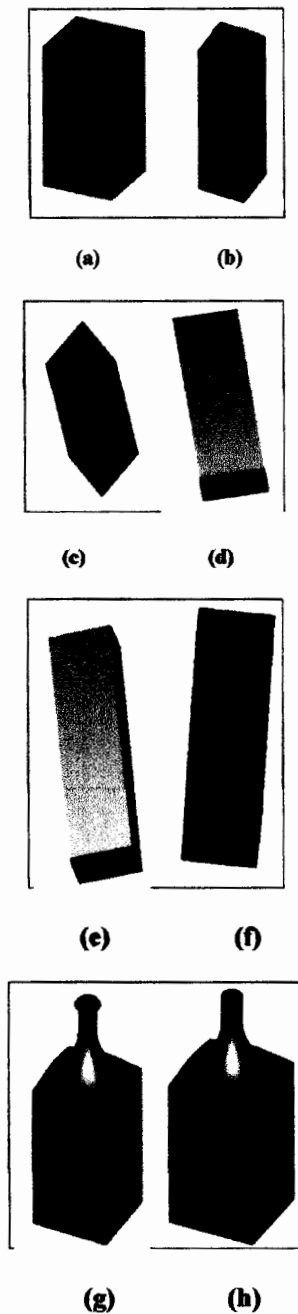
Figure.27 Summary of Fabrication Processes Steps for Hollow Out of Plane Microneedles (a) Silicon Wafer (b) SiO₂ Deposition (c) Backside Etching of SiO₂ (d) DRIE for Needle Channel (e) Depostion of Si₃N₄ (f) Pattern transfer for Front Side (g) Isotropic Etching for Needle Shaft (h) Removal of SiO₂ and Si₃N₄.

6.6 Microneedle Design Dimensions

The obtained hollow out of plane microneedles on process simulator consists of following main design specifications.

    (i)   Silicon wafer thickness = 550 µm

    (ii)   Needle length = 200 µm

    (iii)   Lumen diameter = 40 µm

    (iv)   Center to center spacing between needles = 750 µm

    (v)   Array size = 2 x 4

Symmetric microneedles in form of array are shown in figure 28.
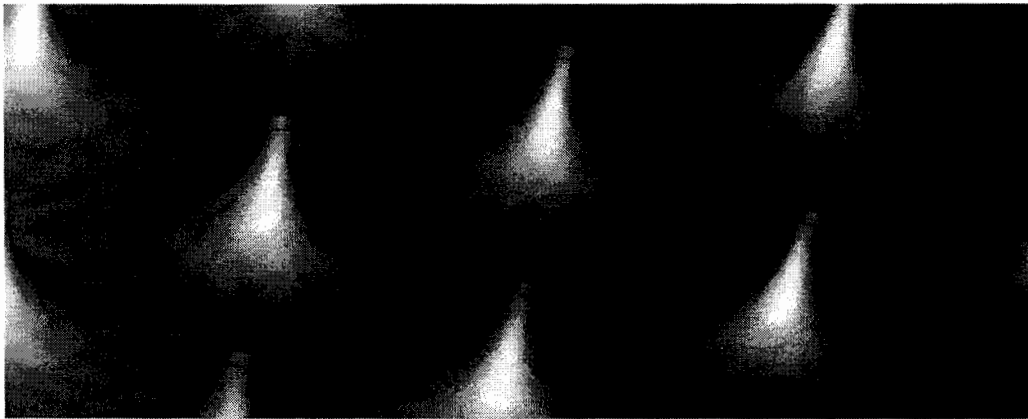
Figure.28 Symmetric Microneedle Arrays

Pointed microneedles in form of array are shown in figure 29.

Figure.29 Pointed Microneedle Arrays

Table.16: **Summary of Hollow Out of Plane Microneedles Fabrication Processes Steps using Process Simulator and General Fabrication Parameters and Techniques.**

PROCESSES STEPS	PROCESS SIMULATOR PARAMETERS / TECHNIQUES	GENERAL PARAMETERS / TECHNIQUES
1. Initial Substrate	Silicon wafer, double sided, 550 μm thickness, <100> orientation.	Silicon wafer, double sided, 550 μm thickness, <100> orientation, doped p-type material.
2. SiO_2 Deposition	Silicon dioxide, 6 μm thickness, deposit conformal, top bottom face.	Silicon dioxide, 6 μm thickness, top bottom side, LPCVD process.
3. Backside Pattern	Silicon dioxide, photolithography, wet aniso etching, bottom face, 40 μm diameter hole.	Silicon dioxide, backside, 40 μm diameter hole, photolithography, plasma etcher.
4. DRIE	Silicon, from bottom face upto 556 μm depth, dry etching.	Silicon, bottom side upto 556 μm depth, DRIE using ICP etching tool.
5. Si_3N_4 Deposition	Silicon nitride, 4 μm thickness, deposit conformal, top bottom face along with needle channel.	Silicon nitride, 4 μm thickness, top bottom side along with needle channel, LPCVD process.
6. Frontside Pattern Transfer	SiO_2 and Si_3N_4, , photolithography, outside mask type, top face with 10 μm depth .	SiO_2 and Si_3N_4 frontside, photolithography, plasma etcher.
7. Isotropic Etching	Silicon, wet iso etching, top face, 200 μm depth with 10 μm undercut.	Silicon, 200 μm depth, plasma etch using ICP etching tool.
8. Removal of SiO_2 and Si_3N_4	SiO_2 and Si_3N_4 , sacrificial etch	SiO_2 and Si_3N_4, concentrated hydrofluoric acid (HF).

DESIGN EXPERIMENTS II –

PROCESS SELECTION OPTIMIZATION FOR THE FABRICATION OF MICRONEEDLES

7.1 Experimental Tool: TCAD SILVACO:

SILVACO Inc's is an electronic design software company established by Dr. Ivan Pasec in 1984 [80]. This tool offers process simulation and modeling of semiconductor devices with a variety of modeling options [81]. SILVACO TCAD suite tool comprises of Athena and Atlas simulator modules that runs in conjunction with interactive tool such as, TONYPLOT, MASK VIEW, OPTIMIZER and DECKBUILD [81, 82] as shown in figure 30. These tools are mainly provided with entire process steps which are primarily needed for the semiconductor device fabrication [81, 82]. These process steps are subsequently supported by empirical and physical models which explain the characteristics of semiconductor processes. [81, 82]

7.2 Key features of TCAD SILVACO

The key features of TCAD SILVACO are as follows [81, 82]:

> ➢ SILVACO ATHENA process simulator offer the facility of physical process based simulations to optimized the structure and design of the devices.

> ➢ Deckbuild interactive tool provided with capability to interconnect among different simulators with backup history functions.

➢ Provided with user friendly environment which easily allows designing, running and debugging the process and device parameters in a real time environment.

➢ ATLAS device simulator envisaged the electrical characteristics of the design device by invoking the device parameters.

➢ The results of the device are represented in contours along with scientific visualization in terms damage profile.
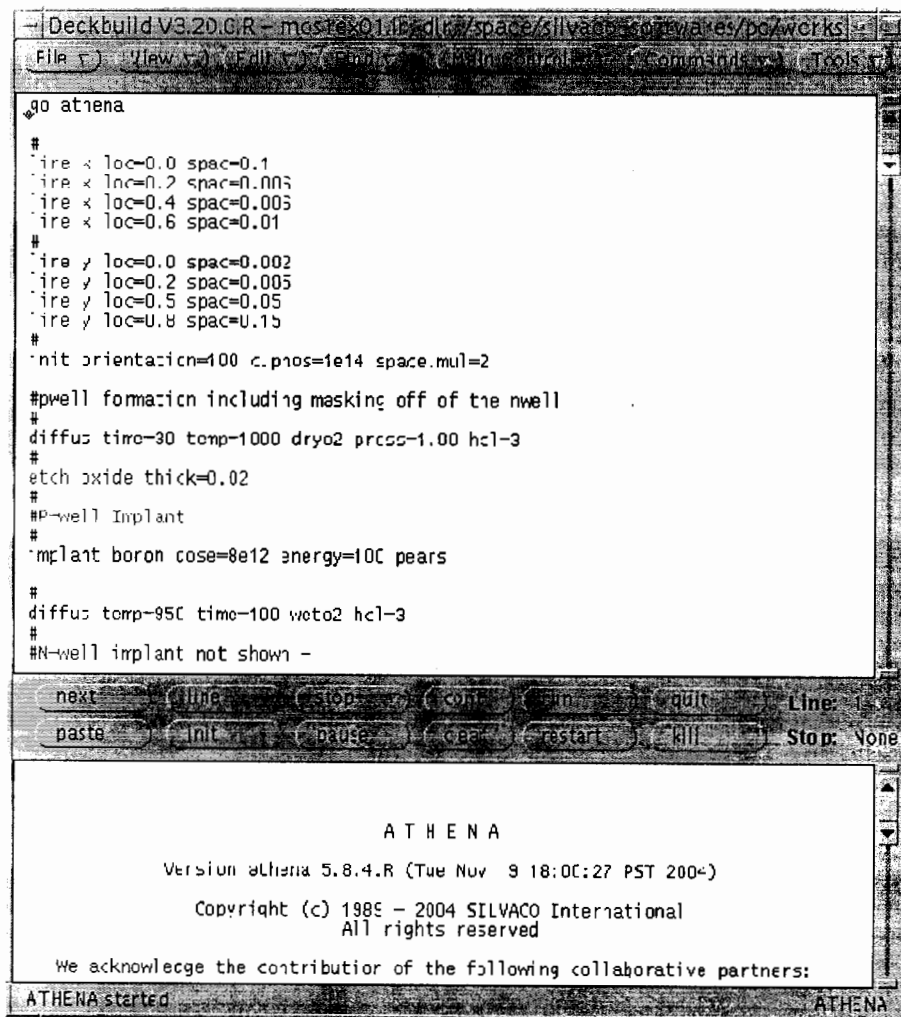
Figure.30 ATHENA Deckbuild Command Window

7.3 Broader Process Parameters Steps (SILVACO) Specific to Si-CMOS fabrication (Fab) Line

Process simulator ATHENA given by SILVACO TCAD [80] has been used for the fabrication of microneedles to gain optimized process selection parameters. Since the SILVACO is primarily based on Si-CMOS processes, therefore the processes fabrication steps for microneedles simulated is slightly different from the processes fabrication steps design on MEMS PRO design tool. This in turn facilitates the device design engineer to make the fabrication and batch production of MEMS based microneedles easy, cost effective, reliable and flexible on standard Si-CMOS fab lines, without altering the experimental set up a great deal. The processes used in SILVACO are invoked by simple physical process parameters rather than using machine parameters. The process steps along with process parameters options for the optimized fabrication of microneedles are provided in the following steps. The selection of the optimized process parameters and final design shapes (refer to figures 30 to 40) are based on numerous routines run on the simulator and in close proximity of the design maintained in MEMS PRO, detailed in chapter 6.

STEP I

The first step is the selection of appropriate substrate or material and preferred material is silicon as shown in figure 31. The optimized parameters options for silicon substrate are given in table 17:

Table.17 Optimized parameter selection for Silicon Substrate

PROCESS PARAMETERS	SELECTION MODES	OPTIMIZED SELECTION
Substrate:	Silicon	Silicon
Orientation:	<100>, <110>, <111> and so on	<100>
Thickness:	1 nm to 750 μm	550 μm
Grown methodology:	CZ, MOCVD, MBE	CZ
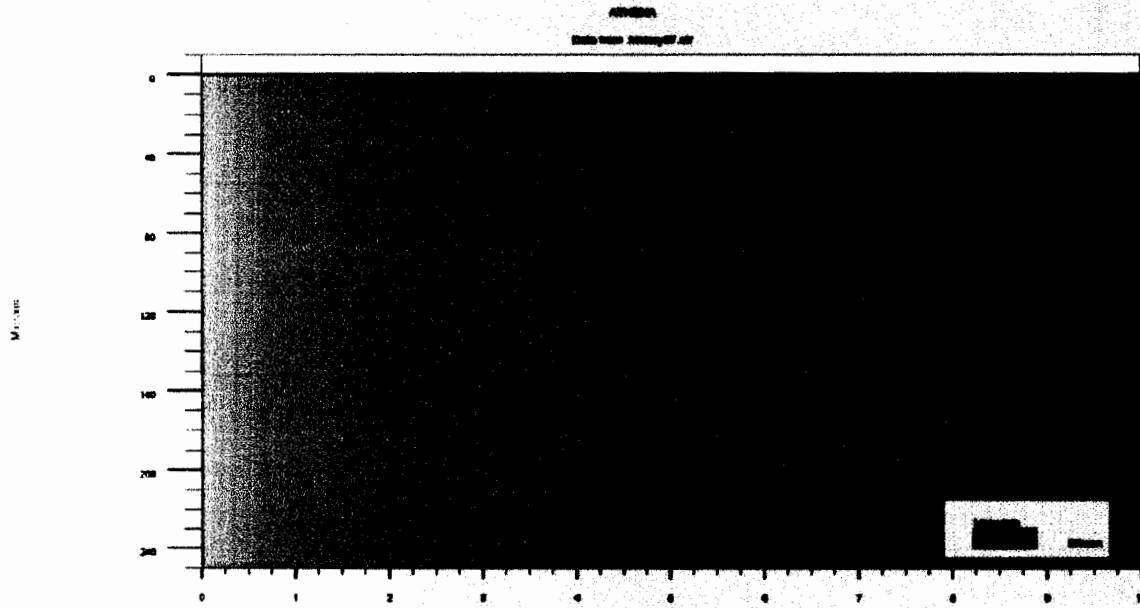
Figure.31 Silicon Substrate

STEP 2

Background doping shown in figure 32, is then carried out in the silicon wafer with p-type boron impurity to modulate its electrical properties and also to provide a region for preferential etch. Optimized parameter options for background doping are given in table 18:

Table.18 Optimized parameter selection for Boron Background Doping

PROCESS PARAMETERS		
Impurity type:	n, p	P - type
Concentration:	1e13 to 1e18 atoms/cm^3	1e13 atoms/cm^3
Initial resistivity:	5 – 10 Ω.cm	6 Ω.cm
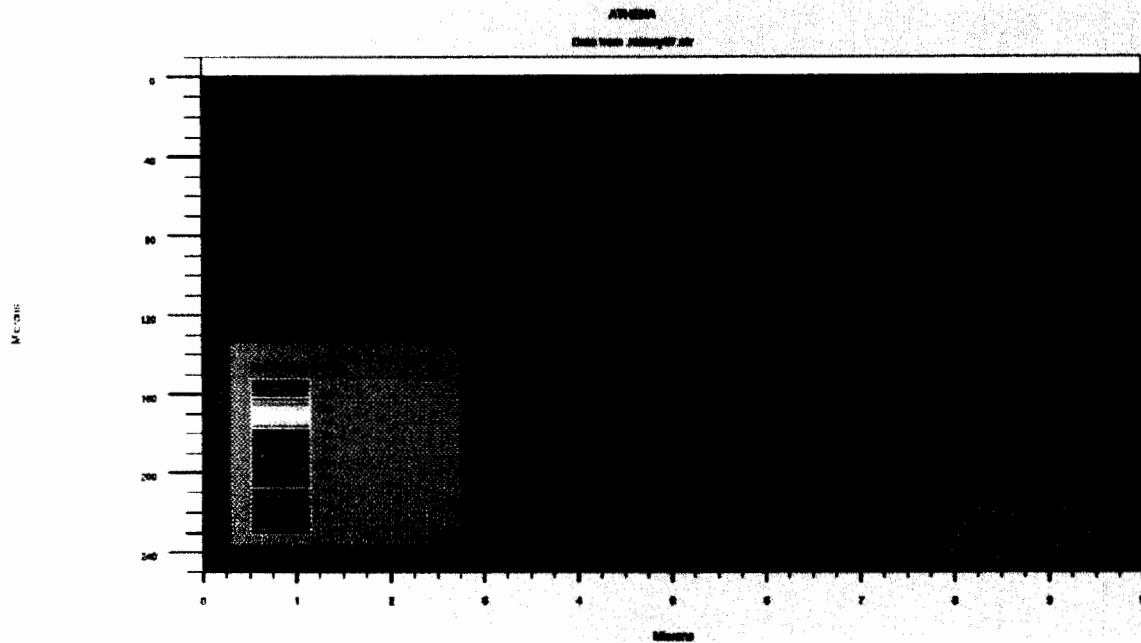
Figure.32 Boron Background Doping

STEP 3

Now in order to craft the outer shape of the microneedle at a height of 200 μm shown in figure 33 geometrical etching of silicon is performed by invoking arbitrary points. Other etching parameter options and their optimized parameter options are given in table 19:

Table.19 Optimized parameter selection for Microneedle Outer Shape

PROCESS PARAMETERS	SETTINGS	
Etching types:	Wet etching, Dry etching, Isotropic and Anisotropic etching	Isotropic
Etch method:	Geometrical, Etching machine	Geometrical
Machine etching type:	Wet etch, RIE	------
Wet etch parameter:	Material, Etch rate, Isotropic rate, Time of run	------
RIE parameters:	Etch rate, Isotropic rate, Directional etch, Chemical rate, Divergence, Time of run	-----
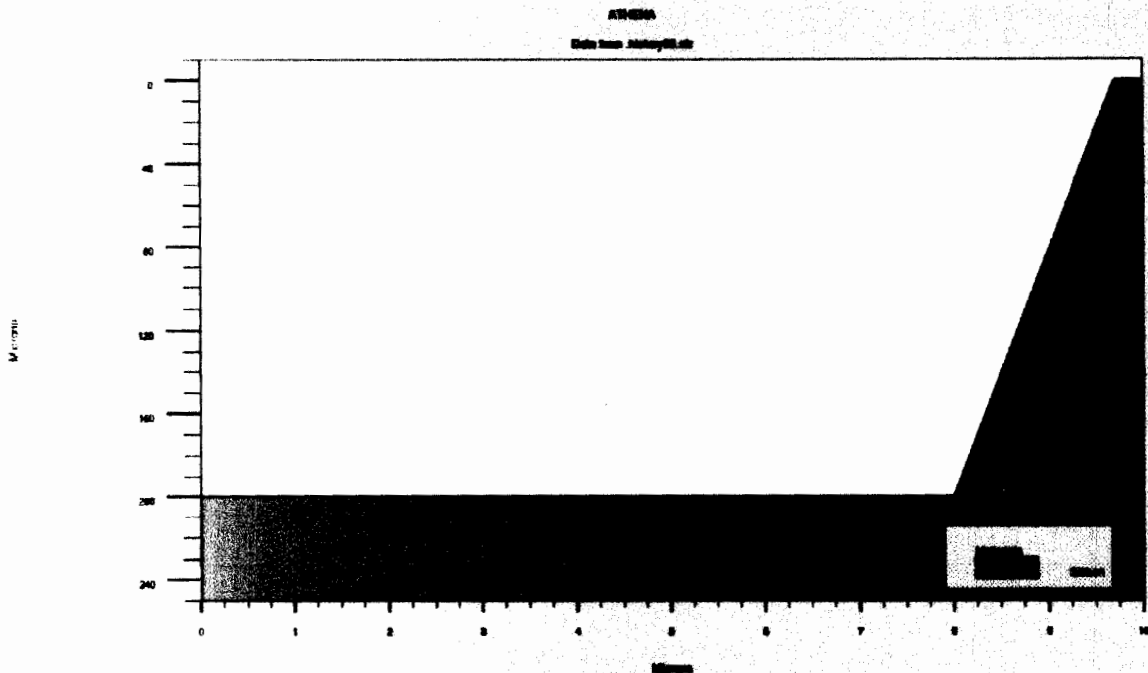
Figure.33 Geometrical Etching for Microneedle Outer Shape

STEP 4

In this step silicon dioxide is thermally grown by dry oxidation in order to protect the side walls and top of the needle shown in figure 34. The other silicon dioxide deposition parameters options and their optimized parameters are given in table 20:

Table.20 Optimized parameter selection for Deposition of Silicon Dioxide

PROCESS PARAMETERS		
Deposit method:	Conformal, Machine	Conformal
Conformal parameters:	Material, Thickness	Material: SiO_2, Thickness: 0.6 μm
Machine type:	LPCVD, PECVD	------
Machine parameters:	Deposition rate, Time of run, Step coverage	------
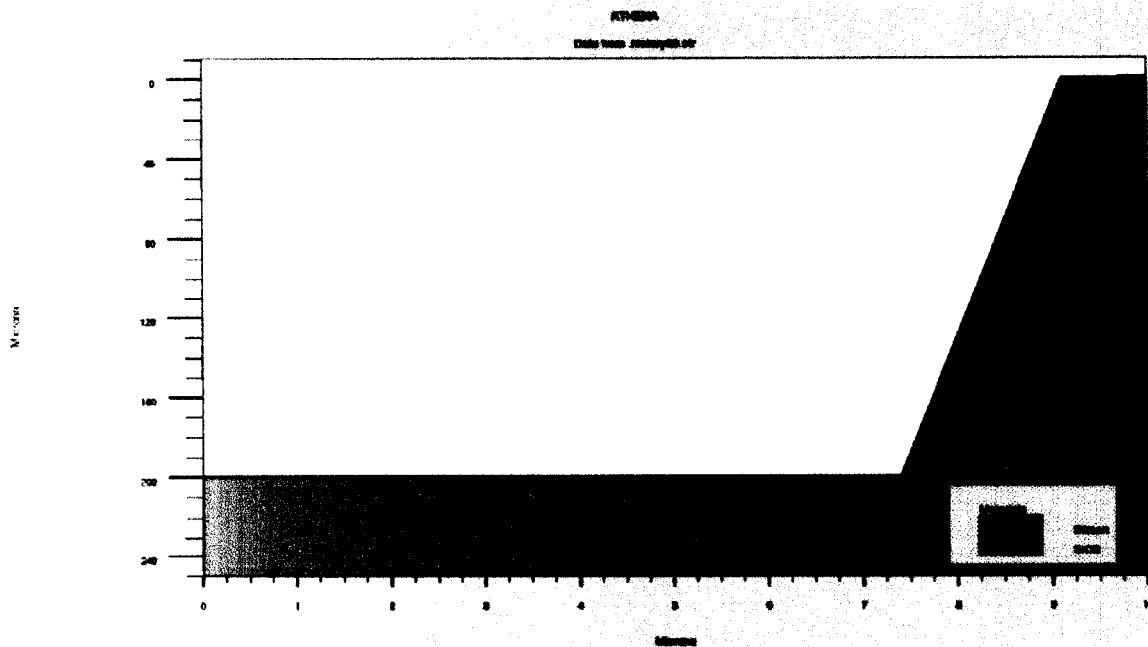
Figure.34 Deposition of Silicon Dioxide

STEP 5

Following the thermal oxidation it is then annealed to strengthen the sidewalls by activating the silicon atoms and also to create a sharp tip of the microneedle during subsequent oxidizing process as shown in figure 35. The annealing parameter options are given in table 21:

Table.21 Optimized parameter selection for Annealing of Silicon Dioxide

PROCESS PARAMETERS		
Time:	25 - 40 min	30 min
Temperature	800 – 1100 C	850 C
Ambient:	Dry oxidation, Wet oxidation, Nitrogen, Gas flow	Dry oxidation
Diffusion Methods:	Fermi, Two dimensional, steady state, and full coupled	Two dimensional
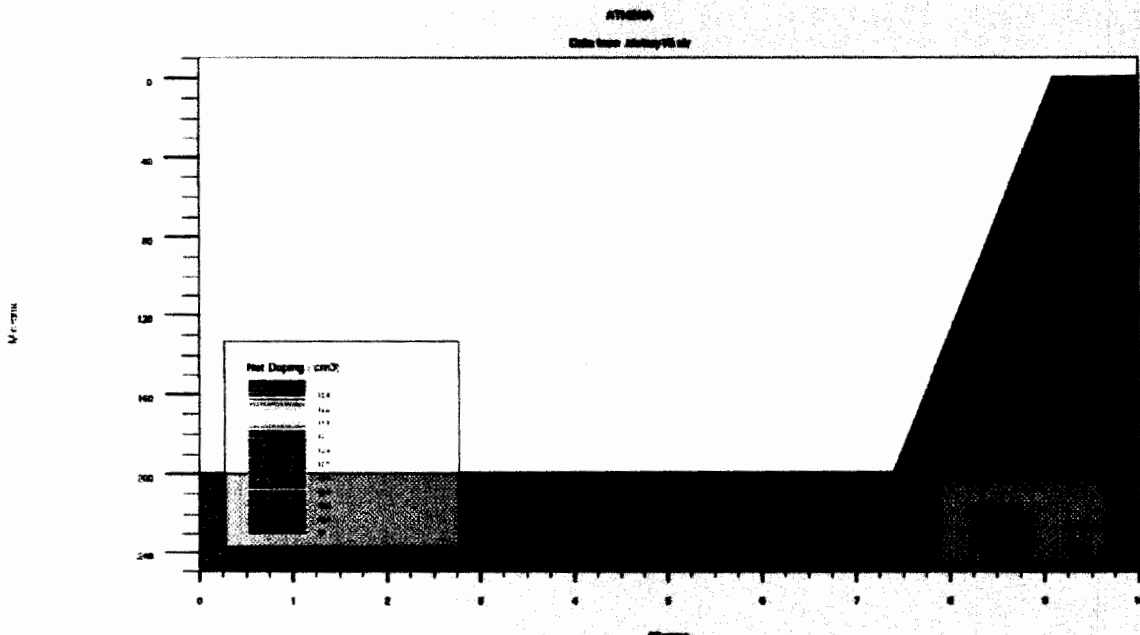
Figure.35 Annealing of Silicon Dioxide

STEP 6

Now the grown silicon dioxide is selectively geometric etched away as shown in figure 36. The remaining portion is covering the needle top. Some of etching parameter selection options is same as given in step 3.
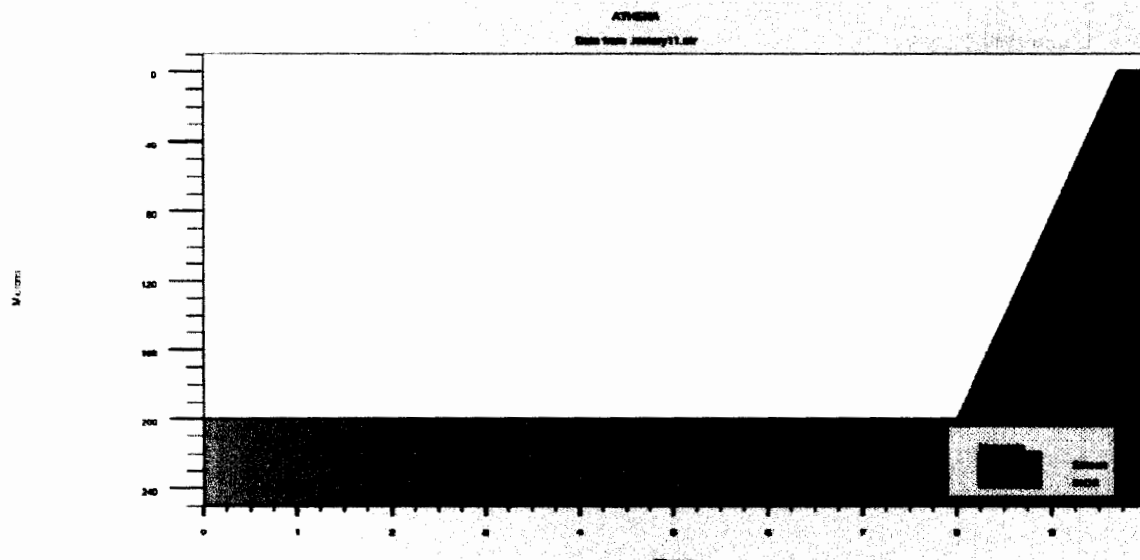
Figure.36 Geometrical Etching of Silicon Dioxide

STEP 7

Silicon nitride (Si_3N_4) is then conformally deposited shown in figure 37 mainly to cover the entire channel of the needle and top of the needle tip. Nitride deposition has same depositions parameter as given in step 4.
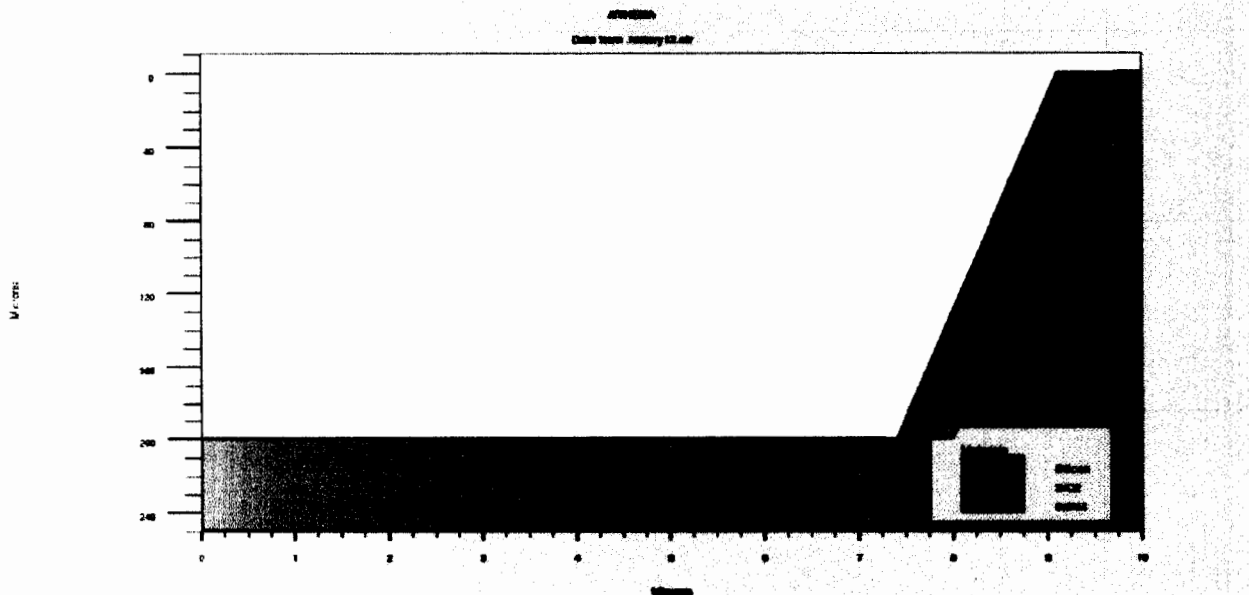
Figure.37 Deposition Silicon Nitride

STEP 8

Nitride is now annealed as can be seen in figure 38 to harden the channel of the microneedle.

Figure.38 Annealing of Silicon Nitride

STEP 9

Now the silicon nitride is selectively geometric etched away as shown in figure 39 remaining on top of silicon dioxide. Some of etching parameter options is same as given in step 3.

Figure.39 Geometric Etching of Silicon Nitride

STEP 10

As a last process, minor steps were performed including mirroring the structure and stripping of remaining silicon dioxide (SiO₂) and silicon nitride (Si₃N₄), as can be seen in figure 40. In the end microneedle with sharp tip shape is formed as shown in contours of the figure 41.
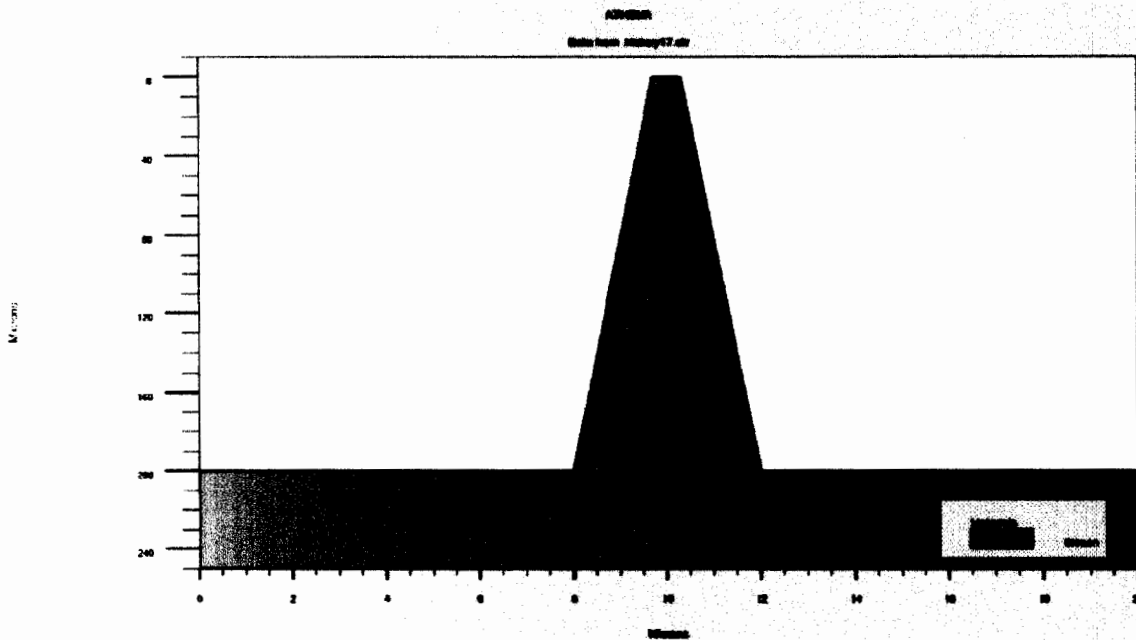
Figure.40 Final Shape of Microneedle
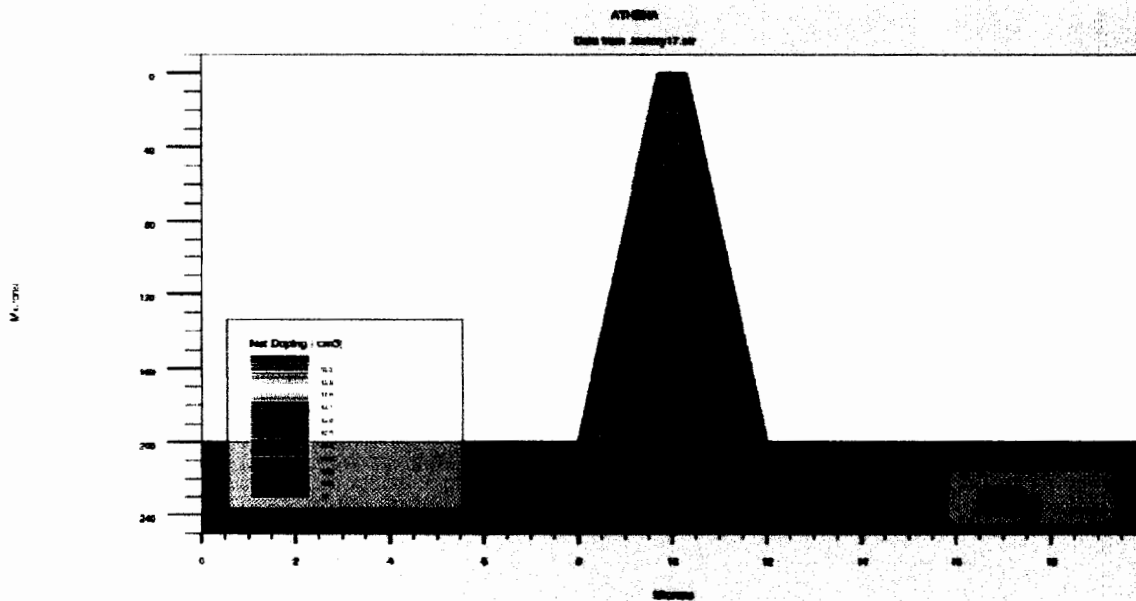
Figure.41 Contour of Final Shape Microneedle with Sharp Tip

7.4 Summary of Processes Simulation for Microneedles on TCAD SILVACO Process Simulator

Figure.42 summarized the fabrication processes of microneedles on TCAD SILVACO based process simulator:
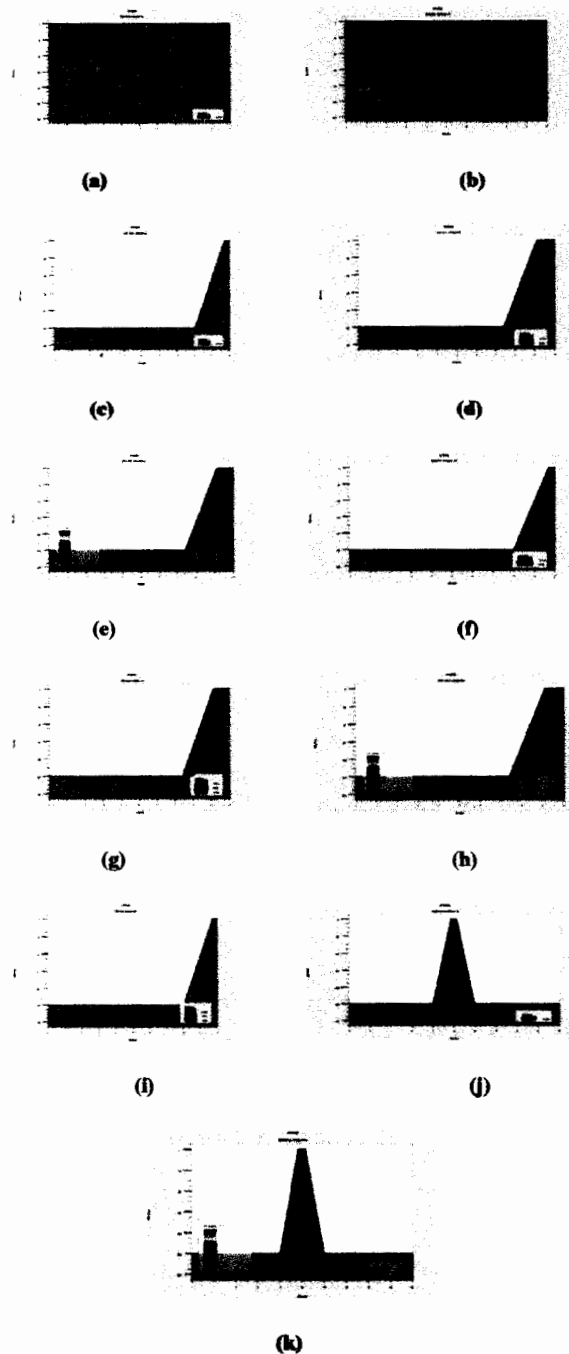
Figure.42 Summary of Process Simulation of Microneedles on SILVACO Process Simulator, (a) Silicon substrate (b) Boron doping (c) Geometrical etching for microneedle outer shape (d) Deposition of SiO₂ (e) Annealing of SiO₂ (f) Geometrical etching of SiO₂ (g) Deposition of Si₃N₄ (h) Annealing of Si₃N₄ (i) Geometric etching of Si₃N₄ (j) Final shape of microneedle (k) Contour of final shape microneedle with sharp tip.

Table.22: - Microneedles Optimized Process Parameters Simulated and design on SILVACO:

PROCESS STEPS	OPTIMIZED PROCESS PARAMETERS
1. Initial Substrate	Material: - Silicon Orientation: - <100> Thickness: - 550 μm
2. Background Doping	Impurity: - Boron (p type) Concentration: - 1e13 atoms / cm^3
3. Etching	Material: - Silicon Etch type: - Geometric etching Geometric method: - Arbitrary points Depth: - 200 μm
4. Deposition	Material: - Silicon dioxide Method: - Conformal Thickness: - 0.6 μm
5. Annealing	Material: - Silicon dioxide Time: - 30 min Temperature: - 850 C Ambient: Dry Oxidation Pressure: - 1 torr
6. Etching	Material: - Silicon dioxide Etch type: - Geometric etching Geometric method: - Left Location: - x=9.70 μm
7. Deposition	Material: - Silicon nitride Method: - Conformal Thickness: - 0.6 μm

8. Annealing	Material: - Silicon nitride Time: - 30 min Temperature: - 850 C Ambient: Nitro Pressure: - 1 torr
9. Etching	Material: - Silicon nitride Etch type: - Geometric etching Geometric method: - Left Location: - x=9.70 μm
10. Minor Steps	Mirror structure right Material: - Silicon dioxide, Silicon nitride Etch type: - Geometric etching Geometric method: - All

DISCUSSION ON SALIENT FEATURES OF RESULTS

8.1 Introduction

The design and simulation results are detailed at length in chapters 6 and 7. Based on the design assessments made and modeling of the underlying mechanics deliberated in chapters 5, we provide an insight to these results in this chapter and discuss them in line with the objectives set forth for this study.

The hollow out of plane microneedle arrays for transdermal drug delivery with needle shaft of 200 μm length and channel diameter of 40 μm were fabricated in the MEMS PRO design tool. These microstructure needles were designed to inject or extract out the drug or fluid from skin via stratum corneum. Mathematical models were re-visited in form of Modified Bernoulli Equations (11) and Extended Modified Bernoulli Equation (12) which are further reduced to equation (26) and equation (39) respectively. These revised models were implemented on MATLAB and simulated for fluid flow characteristics through needles. The physical relationships between several parameters such as flow rate, pressure drop and needle diameters were also developed. Modified Bernoulli Equation was re-visited in such areas where gravitational forces are either considered as negligible or it may ignored sometimes whereas in Extended Modified Bernoulli Equation gravitational forces are taken into consideration, for applications of devised microneedles on ambients where the contribution of gravitation forces are appreciable.

8.2 The contribution of gravitational forces

The gravitational forces were mainly not considered during previous studies of microneedles and treated as negligible during the numerical and experimental analysis of microstructures. In our study the gravitational forces (g) were taken into account during the numerical analysis in order to see its effects on design and flow characteristics of microneedles. During the comparison of

two models, it was found that gravitational force has appreciable impact on geometric aspects of the design and subsequently on its flow characteristics. Gravity is known to have effects and impact on human body as well as on other biological entities, therefore gravitational forces are now also a highly considerable parameter during the design of biomedical systems. This has been a missing link so far, largely in the literature and very little is known on this account. One very recent study published to address this issue partially [83] claimed that during the design of microneedle arrays for biomedical systems, gravitational forces may also be taken into consideration for the transport of drug formulation [83].

8.2.1 Relationship between Pressure Drop and Flow Rate

The pressure drop as a function of flow rate, diameter as a function of flow rate and diameter as function of pressure drop with microneedle geometry has been simulated in our study for an individual microneedle using water as a model liquid with the help of equations (26) and (39). Standard macroscopic values for an edged inlet (K_1= 0.5) and for an exit (K_2= 1.0) were chosen as similar as reference [8, 74] to model the flow characteristics. Other parameters are: L = 550 µm long microneedle lumen [30]. μ = $1.006e^{-3}$ Pa s and ρ = 1000 kg/m^3 were assumed as viscosity and density respectively [30, 61] and g = 9.81 m/s^2 is the standard gravitational value.
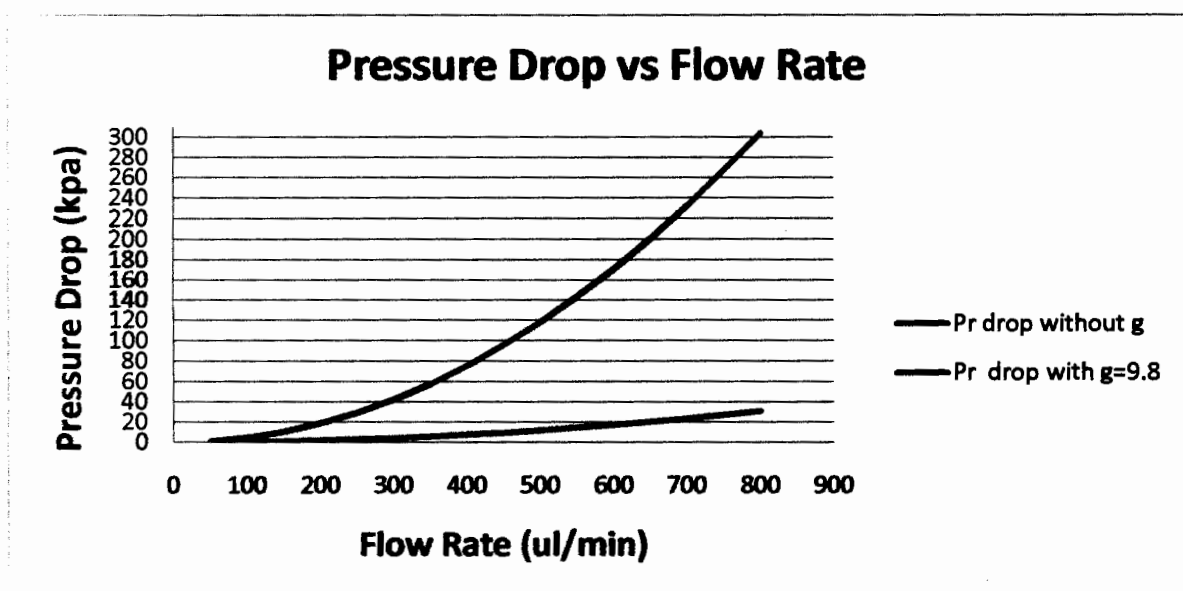
Figure.43 Variation between Pressure Drop and Flow Rate

Figure.43 illustrates the relationship between pressure drop and flow rate simulated at a fixed 40 µm channel diameter of the designed microneedles. From this result, it is noted that diameter of channel is determined by desired flow rate and saturated pressure drop. The curves show that as the flow rate increases, the pressure drop also increases initially for both conditions of "g". The pressure drop however decreases dramatically in case of gravitational force account for as compared to the pressure drop without g. It is due to the physical implication of gravity on the viscous and dense medium and directly impacts the behaviour of pressure dropping due to a certain maintained flow rate within the device.

Form this graph, the diameter that would be used in actual device fabrication would be much smaller when considering the condition of including 'g' in the design analysis. This means when diameter gets smaller, there would be increase in pressure drop and velocity but there values will be relatively smaller as compared to the converse case.

8.2.2 Relationship between microneedle diameter and pressure drop

Figure.44 discusses the relationship between the variations in diameter and pressure drop simulated with constant flow rate at Q = 400 µl/min and 800 µl/min. As the pressure drop increases, the diameter gets decreases in both conditions i-e with and without taking the contribution of g into account. The curves of diameter vs pressure drop are saturated after the drop of pressure reaches a certain value. The diameter of lumen increased with the increased flow rate at certain values of pressure drop which is true for both the conditions. In this graph the curves are becoming flat with the increase of the pressure drop. The region of flattened lines illustrates that the diameter is not very sensitive to the variation of the high pressure drop. Hence a smaller diameter is thus required for the higher pressure drop at the desires flow rate in the microneedless.
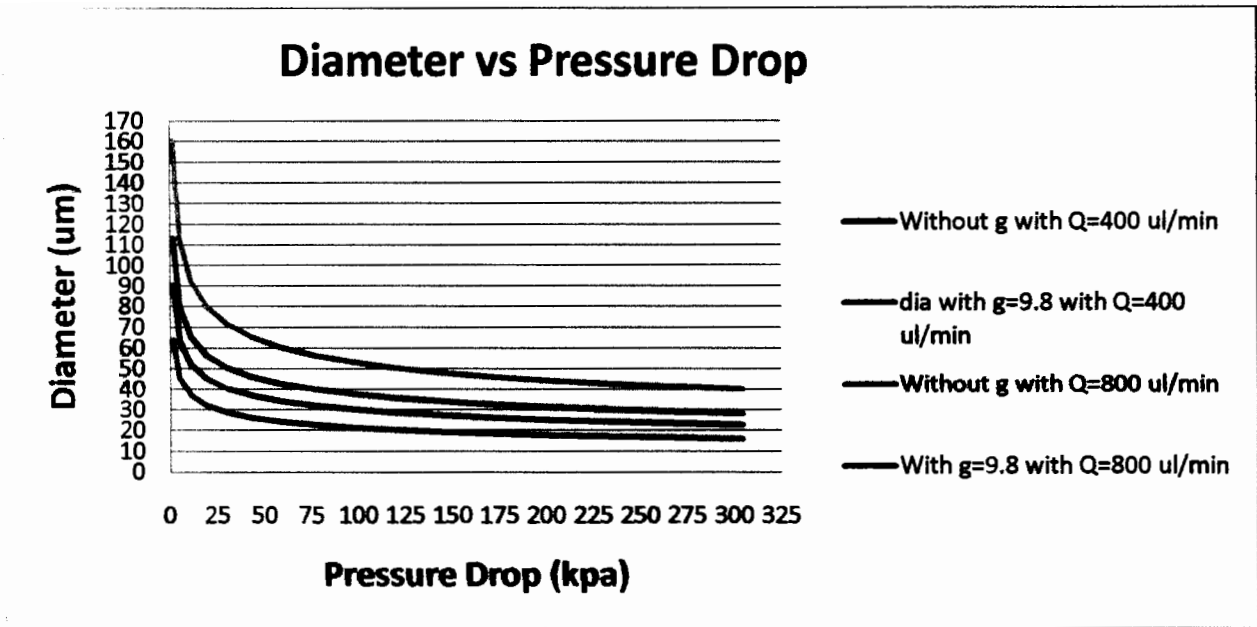
Figure.44 Variation between Diameter and Pressure Drop

It can be noticed that by comparing this graph with both conditions of g the diameter gets much reduced in case where value of "g" is account for contribution of gravitational forces, as compared to the diameter without "g". This also suggests that at a certain value of pressure drop, the increase in the flow rate makes the diameter of lumen also increased.

We gathered from these experiments that the designed diameter of the microneedles can be determined at the saturated region of diameter vs pressure drop curves. The slope of the graph presents the variation of the diameter with pressure drop. After the pressure drop reaches certain a value, the variation of diameter with pressure drop is negligible which is true in both conditions of gravitational forces.

Further, in this graph it also seems that the velocity of flow also go to a decrease with the increase in the diameter, which results in lower pressure drop across a microneedle. Since the water has low viscosity so the flow rate will increase readily. This is true for both conditions of "g". However, the values become smaller for all above parameters when they are compared with the condition where experiments are performed without "g".

8.2.3 Relationship between diameter of the microneedle and flow rate

Figure.45 illustrates the relationship between the variation in the diameter and flow rate simulated with two separate constant pressure drop at 75.9 kpa and 304 kpa. The diameter gets increased with decrease of pressure drop at certain desired flow rate for both conditions of "g". This means that the pressure that is needed to flow the fluid rises dramatically when channel diameter decreases. In this graph, it can further be seen that a very small decrease in the diameter reduces the flow dramatically. This is due to the fact that cross section area (which is directly proportional to the flow rate) gets impacted for both conditions of "g". By comparing the value of diameter with and without the consideration of value of "g", it is found that by including the value of "g" the diameter gets much smaller at higher pressure drop at a desired flow rate, which suggests that there is higher velocity experienced at that particular point.
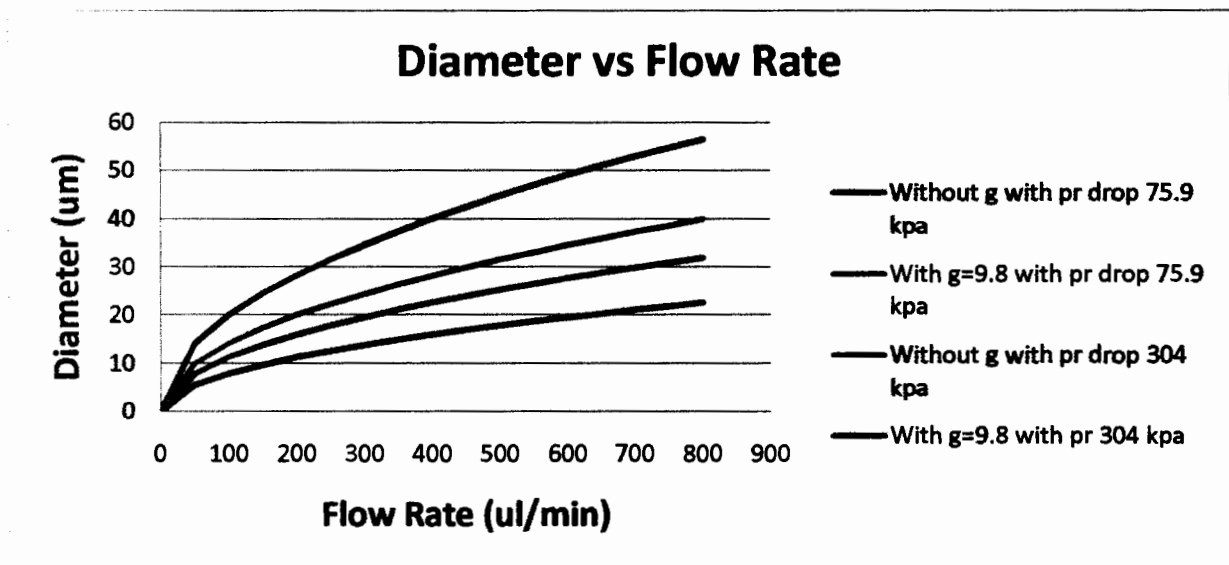
Figure.45 Relationship between Diameter and Flow Rate

8.3 The Geometry of microneedle

The pressure drop is mainly dependent on the geometry of microneedle in combination with fluid viscosity and density for a smooth fluid transportation through microneedle channel. Therefore

appropriate selection of needle geometry leads to an effective biomedical microsystem device. A final design of "symmetric" and "pointed hollow" out of plane microneedles is shown in figure 46. The Deep Reactive Ion Etching (DRIE) is suggested to be performed to create the microneedle lumen. The outside shape of microneedle is suggested to be created by isotropic undercut of silicon dioxide and silicon nitride masks. The obtained microneedle has the following features optimized by the design methods.

(a) Shaft with a wide base and very small thickness of needle tip.

(b) Centerlines of the masks and needle channel leads to the design of symmetric and pointed tip microneedles.

(c) Difference is created in the centerlines of masks and channels which are identical for symmetric micrneedles dislocated by some distance for pointed tip microneedles form one side of the microneedles known as sharp microneedles.

The geometry of the design is adjusted in such away to provide a solution using which a process engineer may fabricate MEMS-based microneedles with the following characteristics:

(a) A miniaturized cross section (controlled by diameter modeling)

(b) A substantial capillary flow rate (controlled by the modeling of pressure drop, contribution of gravitational force and optimized diameter)

(c) Full strength not to break during the skin penetration (controlled by physical process optimization)
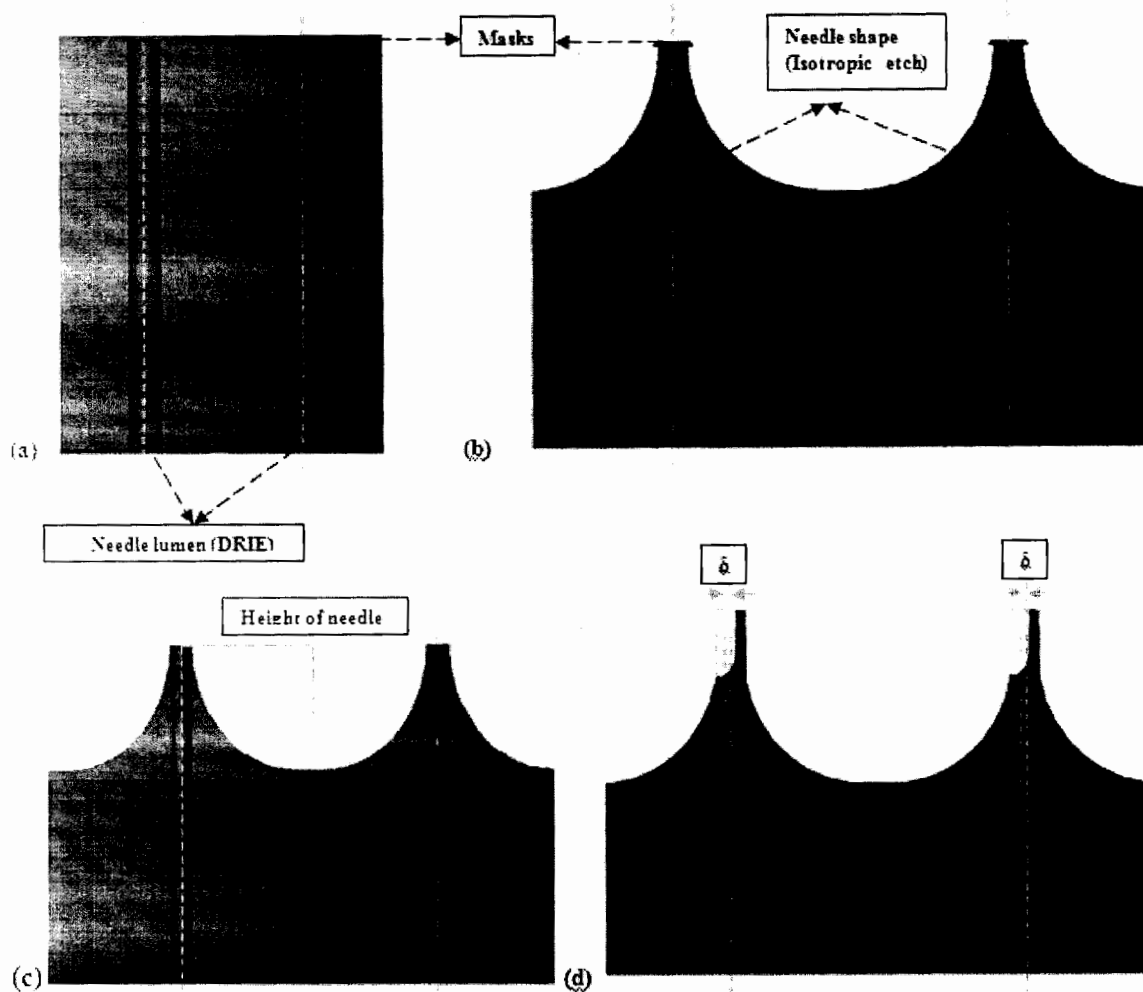
Figure.46 Microneedles Design, (a) Needle Lumen from DRIE, (b) Isotopic Underetched of Masks to create Needle Shape, (c) Symmetric Needle form by the Combination of Centerlines of (a) and (b), (d) Pointed Needle form by Dislocated the Centerlines of (a) and (b) by Distance δ.

8.4 Physical process optimization for fabrication of MEMS-based microneedles

Physical process based simulations has also been carried out to optimize the structure and design of the microneedles. Modelings of the physical processes were performed on the ATHENA process simulator provided by SILVACO. The underlying assumptions and models are governed by the systems of equations that mainly explain the characteristics of engineering chemistry and physics of semiconductor processes [80]. All process steps that are used for the semiconductor devices fabrication are available in the ATHENA process simulator providing an option to the

design engineer to intelligently choose the appropriate process parameters along with selection of physical process itself and run through several iterative simulations to mature the design.

The purpose of the process simulation of microneedles is to predict and manipulate the design structure knowledge that has been obtained after applying specified process steps which was unable to obtain from the MEMS PRO design tool. Since the ATHENA simulator is primarily based on the CMOS fabrication process, the dimensions and design used for microneedles in these simulations are complex, limited in scope relevant to the fab-less solution and cost effective in nature.

The majority of microneedle process steps, as illustrated in chapter 7, are modeled with ELITE tool of the ATHENA simulator that comprises of deposition and etching processes whereas annealing step was performed by applying DIFFUSE parameter in conjunction with time and temperature and two dimensional model of diffusion process. Conformal deposition and geometric etching of ELITE tool has been invoked for the fabrication of 200 μm length of microneedles with sharp tips. The selection of such parameters is purely iterative in behaviour and provides a lot of insight while optimizing the design of MEMS-based microneedles by the optimization of both the modeling and physical process parameters. TONYPLOT [80] provides the results of spatial structure of microneedles with contours along with scientific visualization in terms of damage profile. The insight of TONYPLOT clearly shows the structure of microneedle with sharp tip as shown in figure 40 of chapter 7.

The SILVACO physical process simulator in conjunction with the MEMS PRO tool has been recently utilized by Md. Nurul Abser et al [71] for the first time and showed very promising results. Our study is somewhat different as the utility of both the powerful design and modeling tools for the design and consequent fabrication of MEMS-based microneedles is (a) Focused on the cost effective Si-CMOS fab specific solutions, and (b) focused on physical process parameters rather than machine parameters in TCAD SILVACO environment, which makes it viable for design optimization studies and applications rather than an embedded solution in a mechanical application. A final trade-off (design solution) based on the above discussion is thus presented in figure 47.

```
                    ┌─────────────────────┐
                    │    START PROCESS     │
                    └─────────────────────┘
                               │
                               ▼
                    ┌─────────────────────┐
                    │  INITIAL SUBSTRATE   │
                    │                      │
                    │ SILICON 550um THICK, <100> │
                    └─────────────────────┘
                               │
                               ▼
                            ◇ SiO₂
              NO         DEPOSITION        NO
  ⬭ SNOW FALL  ◀────           ◇            ────▶  ⬭ FILL
                               │
                               │ YES
                               ▼
                    ┌─────────────────────┐
                    │      CONFORMAL       │
                    │                      │
                    │ 6um THICK, TOP BOTTOM FACE │
                    └─────────────────────┘
                               │
                               ▼
                            BACKSIDE
              NO          PATTERN OF        NO
  ⬭ DRY / SACRIFICAL ◀──     SiO₂           ──▶  ⬭ WET ISO
     ETCHING                                        ETCHING
                               │
                               │ YES
                               ▼
                    ┌─────────────────────┐
                    │  WET ANISO ETCHING   │
                    │                      │
                    │ 40um DIAMETER HOLE, BOTTOM FACE │
                    └─────────────────────┘
                               │
                               ▼
                            DRIE FOR
              NO             NEEDLE         NO
  ⬭ WET ANISO / ◀──         CHANNEL        ──▶  ⬭ WET ISO
    SACRIFICAL ETCHING                             ETCHING
                               │
                               ▼
                             (A)
```

A

YES

DRY ETCHING

SILICON FROM BOTTOM FACE UPTO
556um DEPTH

NO ← Si_3N_4 DEPOSITION → NO

SNOW FALL

FILL

YES

CONFORMAL

4um THICK, TOP BOTTOM FACE
WITH NEEDLE CHANNEL

DRY / SACRIFICAL
ETCHING

NO ← FRONTSIDE PATTERN TRNSFER → NO

WET ISO
ETCHING

YES

WET ANISO ETCHING

SiO_2 and Si_3N_4, TOP FACE WITH 10um DEPTH

DRY / SACRIFICAL
ETCHING

NO ← ETCHING FOR NEEDLE SHAFT → NO

WET ANISO
ETCHING

YES

B

84

```
                              ┌─────┐
                              │  B  │
                              └─────┘
                                 │
                                 ▼ YES
    ┌───────────────────────────────────────────────────────┐
    │                  WET ISO ETCHING                       │
    │                                                        │
    │      SILICON, 200um DEPTH WITH 10um UNDERCUT           │
    └───────────────────────────────────────────────────────┘
                                 │
                                 ▼
                            ╱────────╲
    NO                     ╱ STRIPPING ╲                    NO
  ┌──────────────┐  ◄─────┤    OFF      ├─────►  ╭──────────────────╮
  │ DRY ETCHING  │        ╲ MATERIALS  ╱         │  WET ANISO /     │
  ╰──────────────╯         ╲────────╱            │  WETISO ETCHING  │
                                 │                ╰──────────────────╯
                                 ▼ YES
    ┌───────────────────────────────────────────────────────┐
    │               SACRIFICIAL ETCHING                      │
    │                                                        │
    │                  $SiO_2$ and $Si_3N_4$                 │
    └───────────────────────────────────────────────────────┘
                                 │
                                 ▼
                       ┌──────────────────┐
                       │   END PROCESS    │
                       └──────────────────┘
```
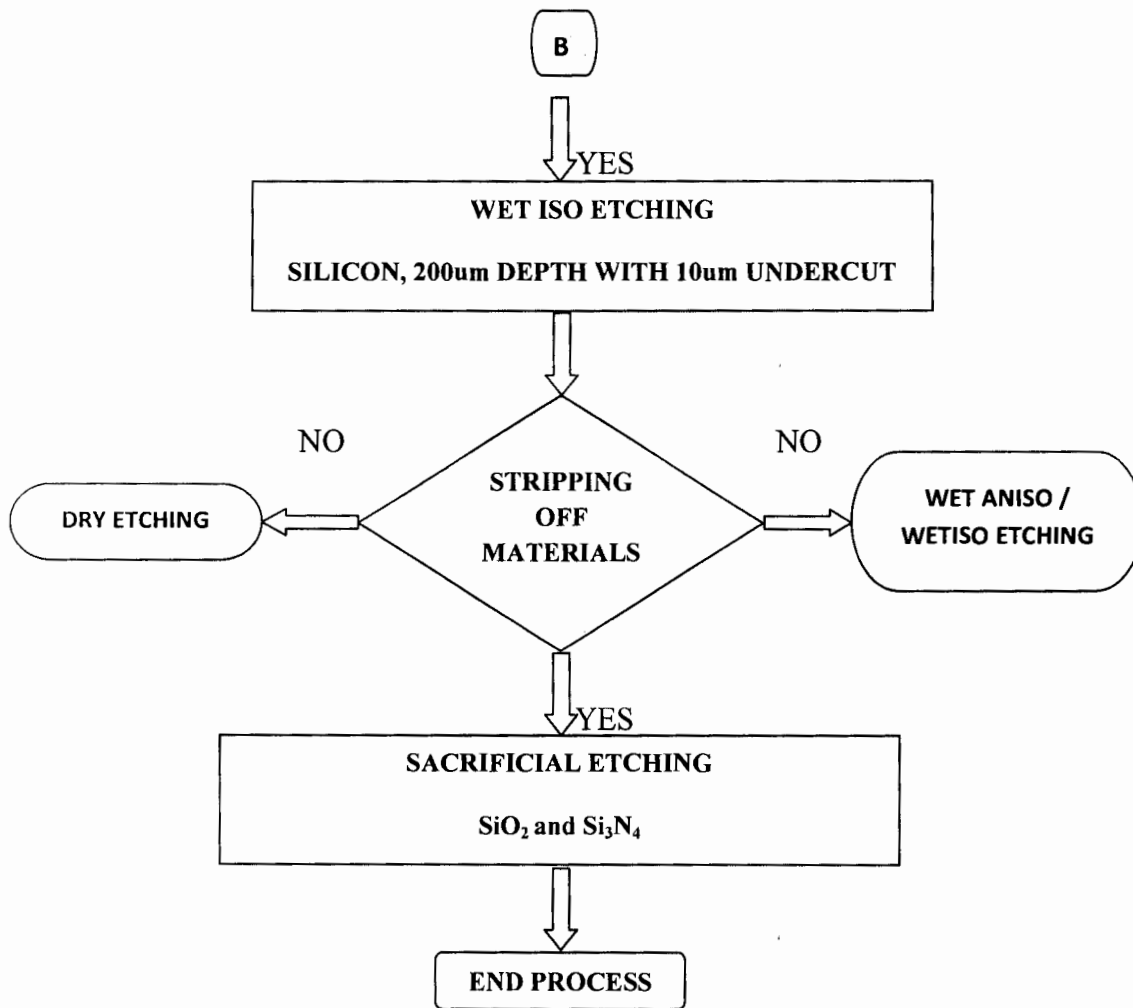
Figure.47 Microneedles Process Flow Chart Design in MEMS Pro Tool

Conclusion and Future Work

9.1 Conclusion

This study was focused to the design and fabrication process of "hollow out of plane" silicon based microneedle arrays for biomedical applications in MEMS environment. The purpose of such microneedles is to offer a design solution which would in turn control physical parameters for a successful painless epidermal drug delivery and cause no trauma at the site. The design of microneedles presented in this work is carried out on the MEMS PRO design in conjunction with TCAD SILVACO process simulation tool. MEMS PRO design tool provided the basic definition of the device whereas TCAD SILVACO was utilized to improve the specific design in line with Si-CMOS fab lines in order to provide a process optimization solution. The major accomplishments of this study are as follows:

➤ The design has been specific to transdermal drug delivery so the dimension of microneedle shaft is set to be 200 um long which may prove to be consequently sufficient to easily penetrate the skin barrier stratum corneum and reach the epidermis. Other dimensions of the suggested design include 40 μm diameter of microneedle channel for fluid transport and 750 μm center to center spacing between the microneedles. These dimensions make the definition of structural design of these microneedles comparable with ones already in use in both commercially and in R&D.

➤ A comparison between mathematical models based on Bernoulli Equation impact and influence of provides useful information regarding the (ignoring and considering) gravitational forces (value of g) on the definition of the design. It is has found that by

considering the value gravitational forces the values get much smaller for diameter, pressure drop, flow rate and other associated parameters, which alter the design of microchannels as well as the characteristics of fluid flow. This may have ramification for design engineers, particularly when using these microneedles in Microsystems operated on altitudes or distinct "g" conditions

- An appropriate selection of microneedle diameter was needed that could deal with the design limitations. With large value of diameters the microneedle channel gets widened which also in turn makes the base of microneedles wider. But for pointed microneedles (our design) with small diameter, sharp tips are created. Therefore diameter with ranges between 35 μm to 45 μm seems suitable for the microchannel created with both types of microneedles.

- Our design also suggests that Deep Reactive Ion Etching (DRIE) is a promising technique to create a buried microchannel for the microneedle, which causes minimal damage to the substrate at the time of etching. Furthermore, keeping the Si-CMOS fab line in view, the isotropic etching is also an applicable etching technique to craft outer shape of needle length from the bulk substrate for the out of plane structures.

- The Bernoulli Equation (and its revisited versions) is a good model for liquid flow through microneedle lumens. This has been established in this study through its verification by incorporating the design considerations in the basic definition of microneedles in MEMS PRO.

- The process simulations on SILVACO ATHENA process simulator have provided an additional advantage to visualize, compare and optimize the physical processes in depth for the potential fabrication of microneedles.

- A trade-off optimization is thus achieved between fab-less and in-fab solutions for MEMS-based microneedles for effective applications in biomedical applications.

9.2 Future Work

Future work can be steered in many directions. Some of the readily available ideas are outlined below.

- ➤ Finite Element Analysis (FEA) or Evolutionary Computing Techniques may be utilized to re-model the underlying physics and mechanics of our designed devices

- ➤ Computational Fluid Dynamics (CFD) may be thought as a sophisticated design methodology for fluidic analysis through microneedles.

- ➤ Reliability and efficacy of designed device may be tested by fabricating these microneedles both in-fab and fab-less environment and characterized by standard strength, flow and efficiency measurements, in real time micro-chip environment. This however demands a commercial run on the process engineer fabrication plants.

REFERENCES

[1] Rashid Bashir, "BioMEMS: state-of-the-art in detection, opportunities and prospects," ELSEVIER, Advanced Drug Delivery Reviews, vol. 56, no.11, pp 1565– 1586, July 2004.

[2] Rajmohan Bhandari, Sandeep Negi , Florian Solzbacher, "A Novel Mask-Less Method of Fabricating High Aspect Ratio Microneedles for Blood Sampling", IEEE Electronic Components and Technology Conference ECTC, pp 1306 – 1309, May 2008.

[3] Rashad Sharaf, Priyanka Aggarwal, KaranV.I.S. Kaler and Wael Badawy, "On the Design of an Electronic Mosquito: Design and Analysis of the Micro-needle", IEEE Proceedings of the International Conference on MEMS, NANO and Smart Systems (ICMENS'03), pp 32 – 35, July 2003.

[4] Nahid Tabassum, Aasim Sofi and Tahir Khuroo, "Microneedle Technology: A New Drug Delivery System", International Journal of Research in Pharmaceutical and Biomedical Sciences, vol 2, no.1, Jan – Mar 2011.

[5] Chin-Chun Hsu, Yu-Tang Chen, Chieh-Hsiu Tsai and Shung-Wen Kangl, "Fabrication of microneedles", IEEE Proceedings of the 2nd International Conference on Nano/Micro Engineered and Molecular Systems, pp 639 – 642, Bangkok, Thailand Bangkok, Thailand, January 2007.

[6] Jooncheol Kim, Seung-Joon Paik, Po-Chun Wang, Seong-Hyok Kim, and Mark G. Allen, "Maskless fabrication of high aspect ratio structures by combination of micromolding and direct drawing", IEEE 24th International Conference on MEMS, pp 280 – 283,Mexico, January 2011.

[7] D.W. Bodhale, A. Nisar, N. Afzulpurkar, "Design, fabrication and analysis of silicon microneedles for transdermal drug delivery applications", Proceedings of the 3rd International Conference on the Development of BME, pp 84 – 88, Vietnam, January 2010.

[8] Boris Stoeber, Dorian Liepmann, "Arrays of Hollow Out-of-Plane Microneedles for Drug Delivery", IEEE Journal of microelectromechanical systems, vol. 14, no. 3, pp 472-479, June 2005.

[9] Bangtao Chen, Jiashen Wei, Francis E. H. Tay , Yee Ting Wong, Ciprian Iliescu, "Silicon microneedle array with biodegradable tips for transdermal drug delivery", Springer Microsystem Technologies, vol 14, no.7, PP 1015- 1019, January 2008.

[10] Jiantao Pan, "MEMS and Reliability", Dependable Embedded Systems, spring 1999. (Available online: http://www.ece.cmu.edu/~koopman/des_s99/mems/)

[11] Prime Faraday Technology Watch, An Introduction to MEMS published by PRIME Faraday Partnership, UK, January 2002.

(Download:http://www.lboro.ac.uk/departments/mm/research/IPMKTN/pdf/Technology_review/ an-introduction-to-mems.pdf)

[12] Tai-Ran Hsu, "Reliability in MEMS packaging", 44th International Reliability Physics Symposium, San Jose, CA, March 2006.

[13] Design guide, Introduction and application areas for MEMS,
Available online:
(http://www.eeherald.com/section/designguide/mems_application_introduction.html.)

[14] Tai-Ran Hsu, Mems and Microsystems Design and Manufacture: Tata McGraw-Hill Publishing Company, 2002

[15] European Union 4th Framework, ESPIRIT Work programme, Sept. 1996.

[16] MEMS and Microsystems in Europe, MCC/WTEC Strategic Technology Tour Report, Published by International Technology Research Institute, section 3, January 2000.

[17] Dirk Beernaert (B), European policy on stimulating Microsystems/MST/MEMS, newsletter on Microsystems and MEMS, mst news, December 1998.

[18] Dr. Klaus Schadow and Dr. Ayman El-Fatatry, "Military/Aerospace MEMS Applications – AVT Task Group 078", RTO AVT Symposium on Novel Vehicle Concepts and Emerging Vehicle Technologies, pp 1 – 50, Belgium, April 2003.

[19] Srinivasa Rao Karumuri, Y.Srinivas, J.Vijay Sekhar , K.Girija Sravani, "Review on Break through MEMS Technology", Archives of Physics Research, 2 (4), pp 158-165, 2011.

[20] Bharat Bhushan, "Nanotribology and nanomechanics of MEMS/NEMS and BioMEMS / BioNEMS materials and devices", ELSEVIER Microelectronic Engineering, vol 84, no.3, pp 387 – 412, March 2007.

[21] (http://www.memsoptical.com/index.htm)

[22] Shekhar Bhansali, Helen Benjamin, Vandana Upadhyay, Nihat Okulan, Kwang Wook Oh, H. Thurman Henderson, Chong H. Ahn, "Modeling Multilayered MEMS-Based Micro-Fluidic Systems", Research summary JOM, pp 57, March 2004.

[23] Yongjun Zhao, Siqi Li, Arthur Davidson, Bozhi Yang, QianWang, Qiao Lin, "A MEMS viscometric sensor for continuous glucose monitoring", IOP journal of micromechanics and microengineering, no.17, pp 2528–2537, November 2007.

[24] M.Mehregany and S.Roy, "Introduction to MEMS ", Microengineering Aerospace Systems. Online: (http://www.aero.org/publications/helvajian/helvajian-3.html)

[25] Henry Helvajian, Microengineering Aerospace Systems: The Aerospace Press, California, 1999.

[26] Microoptics, Sandia National Laboratories,

(Online: http://mems.sandia.gov/about/micro-optics.html.)

[27] MEMS Product List, MEMS Industry Group,

(Online: http://memsblog.wordpress.com/mems-product-list/).

[28] Products, JENOPTIK Optical Systems, Inc,

(Online: http://www.memsoptical.com/index.htm.)

[29] (http://www.memsnet.org/mems/applications.html)

[30] NIDCD Fact Sheet: Cochlear Implants, NIH Publication No. 11-4798, US Updated March 2011.

[31] V. Celeste Carter, Mary Jane Willis, Barbara C. Lopez, "BioMEMS Applications Overview", Participant guide , SCME, May 2010.

[32] James D. Weiland, Wentai Liu, and Mark S. Humayun. "Retinal Prosthesis", Annu. Rev. Biomed. Eng, no. 7, pp 361–401, March   2005.

[33] Teena James, Manu Sebastian Mannoor , and Dentcho V. Ivanov, "BioMEMS –Advancing the Frontiers of Medicine", Review, Sensors, no.8, pp 6077-6107, September 2008.

[34] Tuan Vo-Dinh , Brian Cullum, "Biosensors and biochips: advances in biological and medical diagnostics". Springer-Verlag, Fresenius J Anal Chem , vol 366, Issue: 6-7, pp 540-551. December 2000.

[35] Bio-Chips and Chips for Bio, Report Commissioned by the MEDEA+ Scientific Committee, November 2003. (Downloaad:http://www2.imec.be/content/user/File/Biochips_FinalReport_1_.pdf.)

[36] Chong H. Ahn, Jin-Woo Choi, Gregory Beaucage, Joseph H. Nevin, Jeong-Bong Lee, Aniruddha Puntambekar and Jae Y. Lee, "Disposable Smart Lab on a Chip for Point-of-Care Clinical Diagnostics", Proceedings of the IEEE, vol. 92, no. 1, pp 154-173, January 2004.

[37] The World Book Encyclopedia. Hypodermic injection. In The World Book Encyclopedia;9, pp 480 – 481, World Book Chicago, 1999.

[38] M.S Gerstel and V.A.Place, "Drug delivery device", US 3 964 482 patent 1976.

[39] M. W. Ashraf, S. Tayyaba, N. Afzulpurkar, A. Nisar, Erik LJ Bohez, and A. Tuantranont, "Structural and Microfluidic Analysis of MEMS based Out-of-plane Hollow Silicon Microneedle Array for Drug Delivery", IEEE 6th annual Conference on Automation Science and Engineering, pp 258 – 262, Canada, August 2010.

[40] S. Hashmi, P. Ling, G. Hashmi, M. Reed, R. Gaugler, and W. Trimmer "Genetic transformation of nematodes using arrays of micromechanical piercing structures", BioTechniques, vol.19, pp 766– 770, 1995.

[41] S. Henry, D. V. McAllister, M. G. Allen, and M. R. Prausnitz, "Microfabricated microneedles: a novel method to increase transdermal drug Delivery", Journal of pharmaceutical sciences, vol. 87, no.8, pp 922– 925, August 1998.

[42] Liwei Lin and Albert P. Pisano, "Silicon-Processed Microneedles", IEEE Journal of microelectromechanical systems, vol. 8, no. 1, pp 78 - 84 March 1999

[43] Boris Stoeber , and Dorian Liepmann, "Fluid injection through out-of-plane microneedles", IEEE 1st Annual International EMBS Special Topic Conference on Microtechnologies in Medicine & Biology, France October 2000.

[44] P. K Campbell, K. E. Jones, R. J. Huber, K. W. Horch and R. A. Normann, "A silicon-based, three dimensional neural interface: manufacturing processes for an intracortical electrode array", IEEE Trans Biomed Eng , vol.38, no.8, pp.758-768, August 1991.

[45] Niclas Roxhed, T. Christian Gasser, Patrick Griss, Gerhard A. Holzapfel, Goran Stemme, "Penetration-Enhanced Ultrasharp Microneedles and Prediction on Skin Interaction for Efficient Transdermal Drug Delivery", IEEE Journal of microelectromechanical systems, vol.16, no.6, pp 1429 – 1440, December 2007.

[46] T. Shibata, A. Nakanishi, T. Sakai, N. Kato, T. Kawashima, T. Mineta, and E. Makino, "Fabrication andmechanical characterization of microneedle array for cell surgery", The 14th International Conference on Solid-State Sensors, Actuators and Microsystems, Transducers & Eurosensors '07, pp 719 – 722 , Lyon, France, June 2007.

[47] Peiyu Zhang, Colin Dalton, Graham A. Jullien, "Design and fabrication of MEMS-based microneedle arrays for medical applications", Springer Microsystem Technologies, vol 15, no. 7, pp 1073 – 1082, May 2009.

[48] Muhammad Waseem Ashraf , Shahzadi Tayyaba, Nitin Afzulpurkar, Asim Nisar, Erik Lucas Julien Bohez, Tanom Lomas, and Adisorn Tuantranont, "Design, simulation and fabrication of silicon microneedles for bio-medical applications", ECTI transactions on electrical eng., electronics, and communications, vol.9, no.1, pp 83 – 91, February 2011.

[49] Pandey Shivanand, Patel Binal, D. Viral, "Microneedles: Progress in Developing New Technology for Painless Drug Delivery", International Journal of PharmTech Research, vol.1, no.4, pp 1279-1282, Oct-Dec 2009.

[50] Jaydeep D Yadav, Kμmar A Vaidya, Priyanka R Kulkarni, Rajvaibhav A Raut, "Microneedles: promising technique for transdermal drug delivery", International Journal of Pharma and Bio Sciences, vol. 2, no. 1, pp 684-708, March 2011.

[51] E.V. Mukerjee, R.R Isseroff, R.Nuccitelli, S.D. Collins, R.L. Smith, "Microneedle Array for Measuring Wound Generated Electric Fields", IEEE Proceedings of the 28th EMBS annual international conference,2006.

[52] Michael L. Reed, Whye-Kei Lye, "Microsystems for Drug and Gene Delivery", in proceedings of the IEEE, vol. 92, no. 1, pp 56-75, January 2004.

[53] M. W. Ashraf , S. Tayyaba , A. Nisar , N. Afzulpurkar , D. W. Bodhale, T. Lomas, A. Poyai , A. Tuantranont, "Design, fabrication and analysis of silicon hollow microneedles for transdermal drug delivery system for treatment of hemodynamic dysfunctions", Springer Cardiovascular Engineering, vol. 10, no. 3, pp 91-108, August 2010.

[54] P. Zhang and G.A. Jullien, "Modeling and Simulation of Micromachined Needles", Nanotech technical Proceedings of the 2003 Nanotechnology Conference and Trade Show ,vol. 1, pp 510 – 513, 2003.

[55] F.M. Hendriks, "Mechanical Behaviour of Human Skin in Vivo", Koninklijke Philips Electronics N.V, literature review, pp 1-46, July 2001.

[56] Jaakko malm ivuo, Robert plonsey, Bioelectromagnetism Principles and Applications of Bioelectric and Biomagnetic Fields, New York Oxford University Press, edition 1995. (Online http://www.bem.fi/book/27/27.html)

[57] F.J.G. Ebling, R.A.J. Eady, and I M Leigh, Anatomy and organization of human skin, Textbook of Dermatology, Blackwell Scientific Publications, 5th edition, New York 1992.

[58] BinMa, Zhiyin Gan, ShengLiu, "Flexible Silicon Microneedles Array for Micro Fluid Transfer", IEEE 6th International Conference on Electronic Packaging Technology, 2005.

[59] Po-Chun Wang, Seung-Joon Paik, Jooncheol Kim, Seong-Hyok Kim, and Mark G. Allen, "Hypodermic-needle-like hollow polymer microneedle array using UV lithography into micromolds", IEEE 24th International Conference on MEMS, pp 1039 – 1042,Mexico, January 2011.

[60] Buddhadev Paul Chaudhri, Frederik Ceyssens, Piet De Moor, Chris Van Hoof and Robert Puers, "A high aspect ratio SU-8 fabrication technique for hollow microneedles for transdermal drug delivery and blood extraction", IOP Journal of micromechanics and microengineering 20, pp 1 – 6, June 2010.

[61] Yu-Tang Chen, Chin-Chun Hsu, Chieh-Hsiu Tsai, and Shung-Wen Kang, "Fabrication of microneedles", Journal of Marine Science and Technology, vol. 18, no. 2, pp. 243-248, 2010.

[62] Seung-Joon Paik, Seong-Hyok Kim, Po-Chun Wang, Brock A. Wester, and Mark G. Allen, "Dissolvable-tipped, drug-reservoir integrated microneedle array for transdermal drug delivery", IEEE 23rd International Conference on MEMS, pp 312-315, January 2010.

[63] Ciprian Iliescu, Bangtao Chen, Jiashen Wei, Zhilian Yue, "Transdermal drug delivery: microfabrication insights", IEEE International semiconductor conference, pp 203 - 209, CAS, November 2009.

[64] Bangtao Chen, Jiashen Wei, Francis E. H. Tay, Yee Ting Wong, Ciprian Iliescu, "Silicon microneedle array with biodegradable tips for transdermal drug delivery", Design, Test, Integration and Packaging (DTIP) of MEMS/MOEMS,EDA publishing, Italy, April 2007.

[65] Po-Chun Wang, Brock A. Wester, Swaminathan Rajaraman, Seung-Joon Paik, Seong-Hyok Kim, and Mark G. Allen, "Hollow Polymer Microneedle Array Fabricated by Photolithography Process Combined with Micromolding Technique", IEEE 31st Annual International Conference of EMBS, pp 7026 – 7029, USA, September 2009.

[66] Puneet Khanna, Kevin Luongo, Joel A Strom and Shekhar Bhansali, "Sharpening of hollow silicon microneedles to reduce skin penetration force", IOP Journal of micromechanics and microengineering, 20, pp 1 – 8, March 2010.

[67] G. Barillaro, A. Diligenti, L. M. Strambini, "Silicon Dioxide Microneedles for Transdermal Drug Delivery", IEEE SENSORS Conference, pp 1104 – 1107, December 2008.

[68] Jung-Hwan Park, Yong-Kyu Yoon, Seong-O Choi, Mark R. Prausnitz, and Mark G. Allen, "Tapered Conical Polymer Microneedles Fabricated Using an Integrated Lens Technique for Transdermal Drug Delivery", IEEE Transactions on biomedical engineering, Vol. 54, No. 5, pp 903 – 913, May 2007.

[69] Sangchae Kim, Smitha Shetty, Dorielle Price, and Shekhar Bhansali, "Skin Penetration of Silicon Dioxide Microneedle Arrays", IEEE Proceedings of the 28th EMBS Annual International Conference New York City, USA, pp 4088 – 4091, Aug 30-Sept 3, 2006.

[70] Md. Shofiqul Islam, Md. Nurul Abser, Md. Nurul Islam and Md. Tanjil Shivan, "Realization of high aspect ratio silicon microneedles using optimized process for bio medical applications", IEEE TENCON, pp 1 – 5 , January 2009.

[71] Md. Nurul Abser, "Solid Silicon Microneedles for Safe and Effective Drug Delivery to Human Eye", Journal of Electrical Engineering, the Institution of Engineers, vol. EE 36, no. II, pp 28 – 34, Bangladesh, December 2009.

[72] Wikipedia, (http://en.wikipedia.org/wiki/Bernoulli's_principle)

[73] (http://iamechatronics.com/notes/78-lessons-in-instrumentation/399-fluid-mechanics-bernoullis-equation)

[74] W. S. Janna, Design of Fluid Thermal Systems. Boston, MA: PWS Kent Publishing Company, 1993.

[75] Chapter 12,"Bernoulli Equation and Energy Equations", McGraw Hill Higher Education, pp 471 – 503.
Download:
(http://highered.mcgraw-hill.com/sites/dl/free/0073380202/903327/Sample_Chapter.pdf)

[76] Wikipedia, (http://en.wikipedia.org/wiki/Darcy%E2%80%93Weisbach_equation)

[77] Batchelor, G.K, "An Introduction to fluid dynamics", Cambridge University Press, Cambridge, 1967.

[78] SoftMEMS, MEMS PRO user guide.

[79] Online: (http://www.softmems.com/mems_pro.html)

[80] Wikipedia, (http://en.wikipedia.org/wiki/Silvaco)

[81] SILVACO ATHENA user's manual. Online (www.silvaco.com)

[82] http://www.silvaco.com/products/interactive_tools/interactive.html

[83] VadimV.Yuzhakov, "Microneedle array, patch and applicator for transdermal drug delivery", US. Patent 7,658,728 B2, Feb.9, 2010.